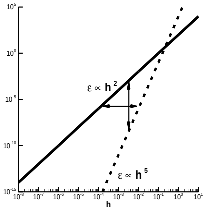

High-Order Method Development at Langley: Past , Present and Future

NASA Langley Research Center
Computational Fluid Dynamics Peer Review

Mark H. Carpenter
Computational AeroSciences Branch

01/28/10

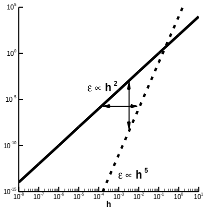

Outline

- Why High-Order / History / Impediments
- “Current” Langley Activity
  - Discontinuous Galerkin
  - Energy Stable WENO
- Questions

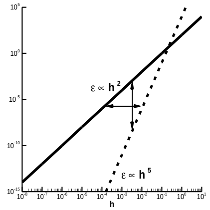

Why High-Order Methods (HOM)

- Problems are quickly getting larger and unsteady
    - Model whole tunnel with sting
    - Unsteady fluid-structures interaction
- Kreiss and Oliger: $u_t + au_x = 0$, $u(x,0) = e^{(i\,kx)}$ ===>>>> $\epsilon(k) = [\beta\, k\, a\, T_f (\frac{2\pi}{P})^p]$
    - P = points/wavelength; T_f = final time; beta = constant ; p = polynomial order

- LES of wing, Re = 10^7:
    - "Grand Challenge" in 4 decades

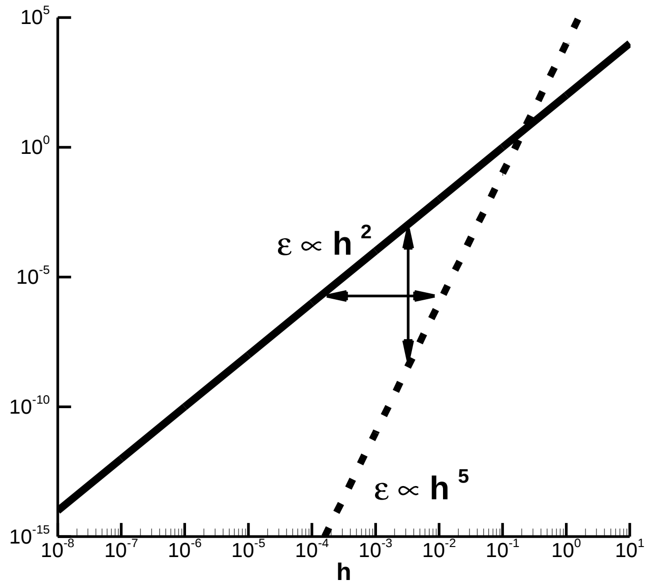

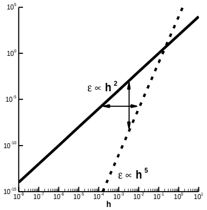

How Mature is CFD?

(6 orders already; How many more?)

- DISCRETIZATIONS : 2 => 2 ½ orders
  - High-Order spatial operators yield 1 ½ => 2 orders improvement
    - Limiters / Solvers / Grid adaptation
  - High-Order temporal operators could yield ½ order of improved efficiency
    - Automated integration with 4th- order methods
      - Temporal error estimators / Variable timestepping
  - Local complement : 1 1/2 FTE (i.e. Langley CS/Contractor, NIA, . . .)
- SOLVERS: 1 ½ => 2 orders
  - Far from optimal but far from easy! Slow progress.
  - Local complement : 1 FTE
- GRID ADAPTION : 2 orders
  - Adjoint error estimators
  - Local complement : 1 FTE
- David Keyes (Columbia) & Steven Jardin (Princeton): similar est!

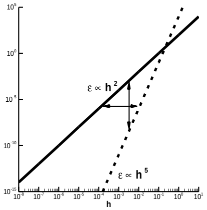

Barriers and Challenges for HOMs

- Circa 2010
  - Discontinuous solutions
    - Unresolved features, bad grids, . . .
    - Mathematical foundation not as mature
    - 95% robustness test
  - Efficient Solvers
    - Inherent stiffness of discrete operator
    - Indefinite nature of matrices
    - Lack inevitable fine-tuning of algorithms
    - Analysis (e.g. Unstructured methods)

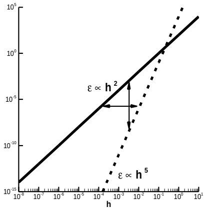

High-Order Methods at Langley
Past: A Long and fruitful history!

- Applications driving HO method use and development
  - Transition onset prediction and control
  - Turbulence modeling and control
  - Noise prediction and control
  - Airfoil design
  - DNS (temporal / spatial) and LES
- Langley Developers / Users
  - Atkins, Balakumar, Carpenter, Casper, Choudhari, Chang, Kumar, Li, Harris, Malik, Rudy, Singer, Streett, Vatsa, Watson, Zang . . .
- FY08 and before: Focused HO Method development group (>= 1 FTE)
  - Project funded
- FY09 and after: Distributed development
  - Project funded

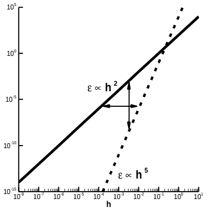

High-Order methods at Langley Present: A new funding Paradigm

- Applications driving HO method use and development: Same
  - –Transition/Turbulence/Noise/Design/DNS/LES
- Current Langley Efforts
  - –CESE; (4th-order CD) : Chang
  - –Vulcan; (ESWENO): Carpenter/White; NN; (DG): Atkins
  - –Overflow; (WENO): Buning
  - –FUN3D; (DG): (K-exact FV):
  - –NoName; (WENO): Balakumar
- Langley External Efforts
  - –Darmofal; MIT Project X; DG-FEM ; Monitor: Atkins
  - –Mavripilis; Wyoming; DG-FEM/ HO-Temporal; Monitor Thomas
  - –Wu; NIA; WENO/DNS; Monitor Choudhari
  - –Fasel; Arizona; HO-CD / DNS; Monitor Choudhari
  - –Martin; Princeton; WENO / DNS; Monitor Gnoffo
  - –Zhong/Kim; UCLA; WENO / DNS ; Monitor Choudhari

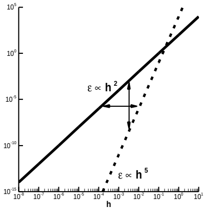

Outline

- Why High-Order / History / Impediments
- “Current” Langley Activity
  - Discontinuous Galerkin (Harold Atkins)
  - Energy Stable WENO
- Questions

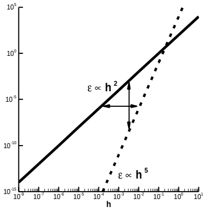

People and Places
15 years of DG at Langley

Lead Discontinuous Galerkin
- Harold Atkins (LaRC)

Contributors
- Chi-Wang Shu and student (Brown U.)
- David Lockard (LaRC)
- David Keyes and student (ICASE, Columbia U.)
- Fang Hu (Old Dominion U.)
- Dimitri Mavriplis (U. Wyoming)
- Brian Helenbrook and student (Clarkson U.)
- Chau-Lyan Chang (LaRC)

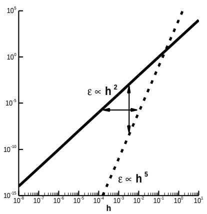

One-Page Summary of Early Work

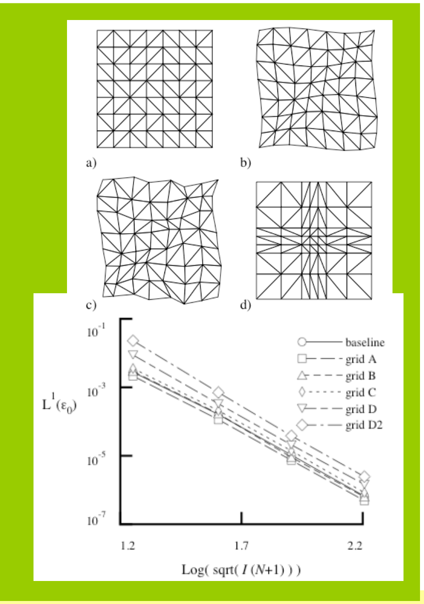

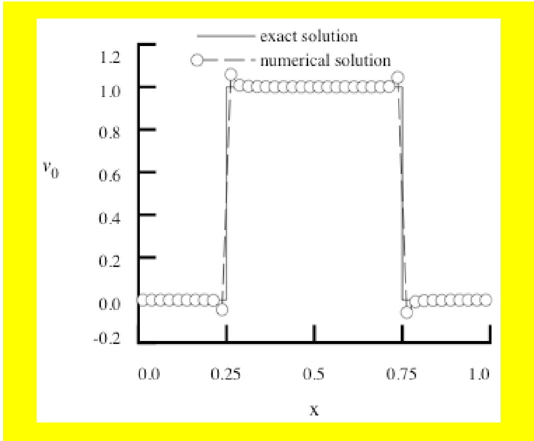

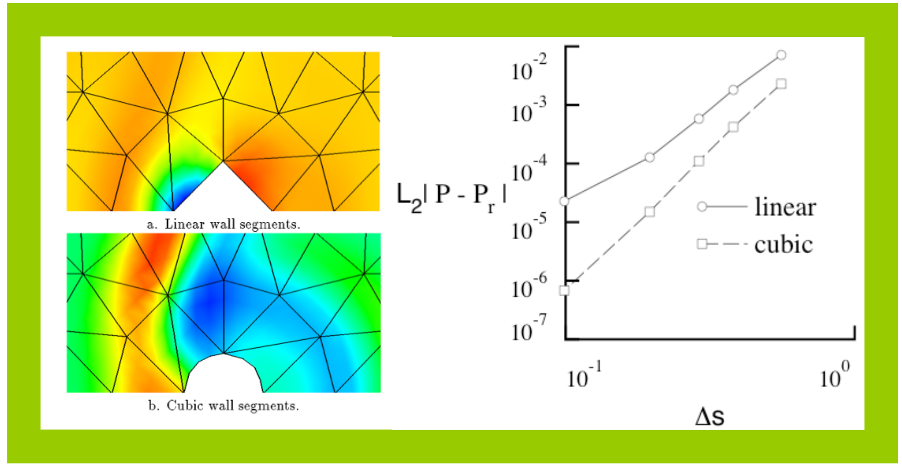

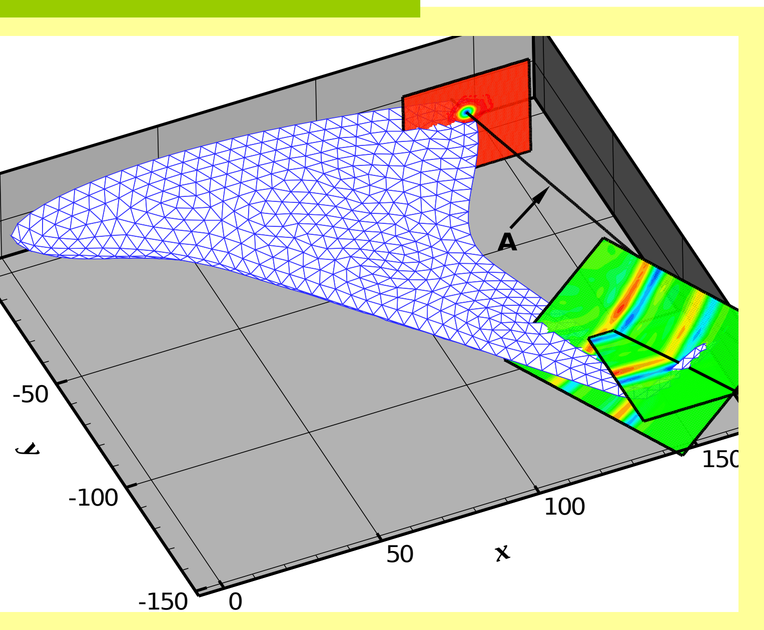

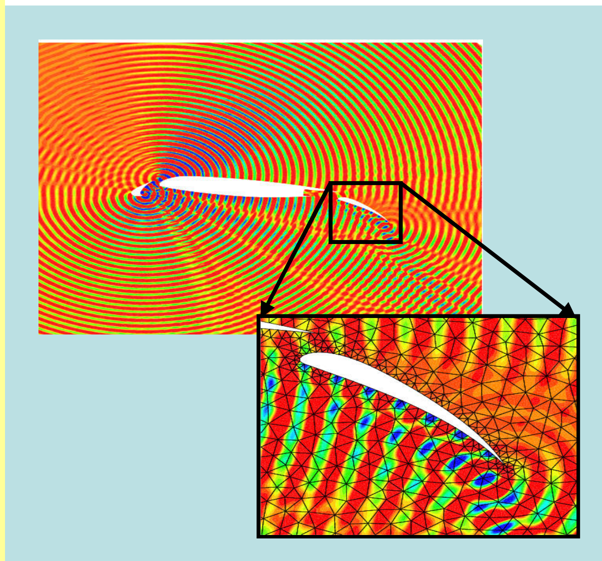

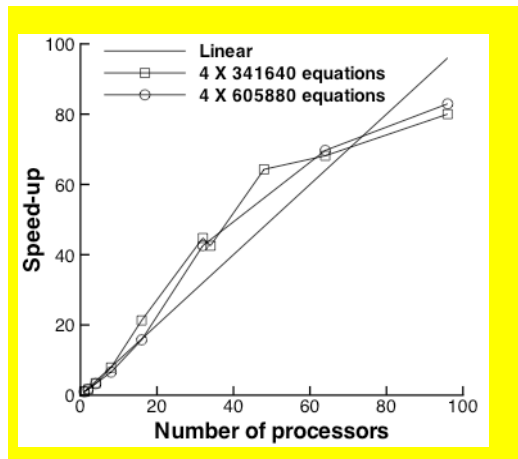

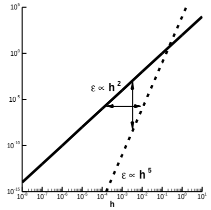

Rate of Grid Convergence and Sensitivity to Mesh Smoothness

Numerical Test

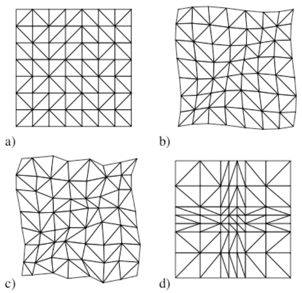

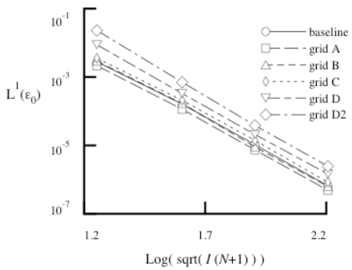

Analysis

assume:

$$\mathbf{u}_h^n(\xi, t) = e^{-i\omega t}\lambda^n P_h(\xi) \quad \text{where} \quad \lambda = e^{iK_h}$$

choose ω, solve for λ

apply interface matching

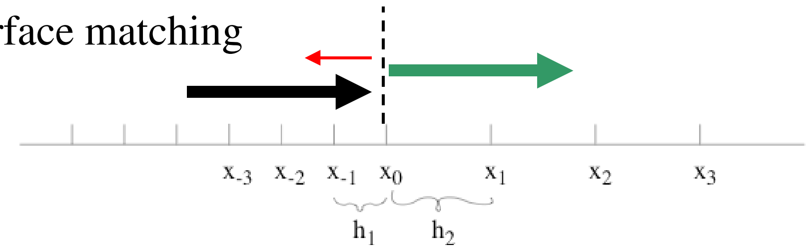

Two Dimensional

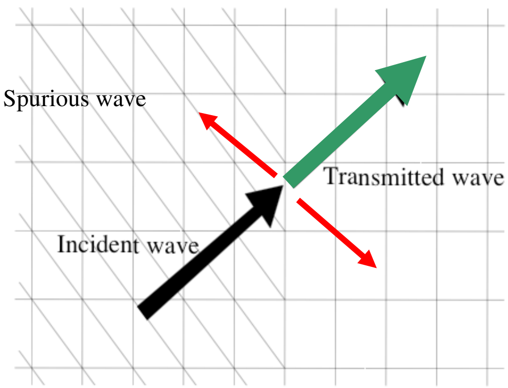

Applicable to:

- change in grid topology
- change in flux function
- change in polynomial order
- boundary conditions

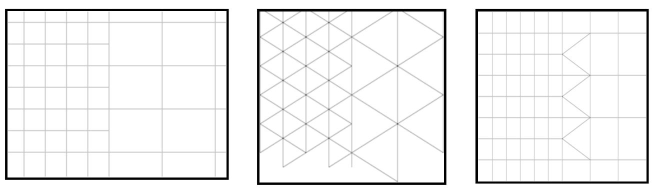

Conclusions:

Spurious modes …

- are highly damped.
- amplitude's converge to zero with order of discretization.

Mesh Smoothness is not an issue

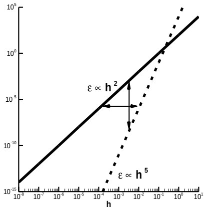

Rate of Grid Convergence continued ...
An Unexpected Finding

assume:

$$\mathbf{u}_h^n(\xi,\, t) = e^{-i\omega t}\lambda^n P_h(\xi) \quad \text{where} \quad \lambda = e^{iK_h}$$

choose ω, solve for λ

$$(1-\gamma)[G(iK)\lambda - H(iK)] + (-1)^{p+1}(1+\gamma)[G(-iK)\frac{1}{\lambda} - H(-iK)] = 0$$

$$\begin{array}{lll}
p=1 \Longrightarrow & G(x) = 1 - \frac{1}{3}x & H(x) = 1 + \frac{2}{3}x + \frac{1}{6}x^2 \\
p=2 \Longrightarrow & G(x) = 1 - \frac{2}{5}x + \frac{1}{20}x^2 & H(x) = 1 + \frac{3}{5}x + \frac{3}{20}x^2 + \frac{1}{60}x^3 \\
p=3 \Longrightarrow & G(x) = 1 - \frac{3}{7}x + \frac{1}{14}x^2 - \frac{1}{200}x^3 & H(x) = 1 + \frac{4}{7}x + \frac{1}{7}x^2 + \frac{2}{105}x^3 \\
 & & \quad + \frac{1}{840}x^4 \\
\cdot & & \\
\cdot & &
\end{array}$$

$$\lambda = \frac{H(iK)}{G(iK)} = \text{ exact Pade approximation of } e^{iK} \text{ to order } 2p+2$$

$$Re(K_h) - K = O^{2p+2} \qquad \text{and} \qquad Im(K_h) = O^{2p+1}$$

super-convergence

-- proven analytically

-- 1D and 2D propagation

DG Discretizations of Navier-Stokes

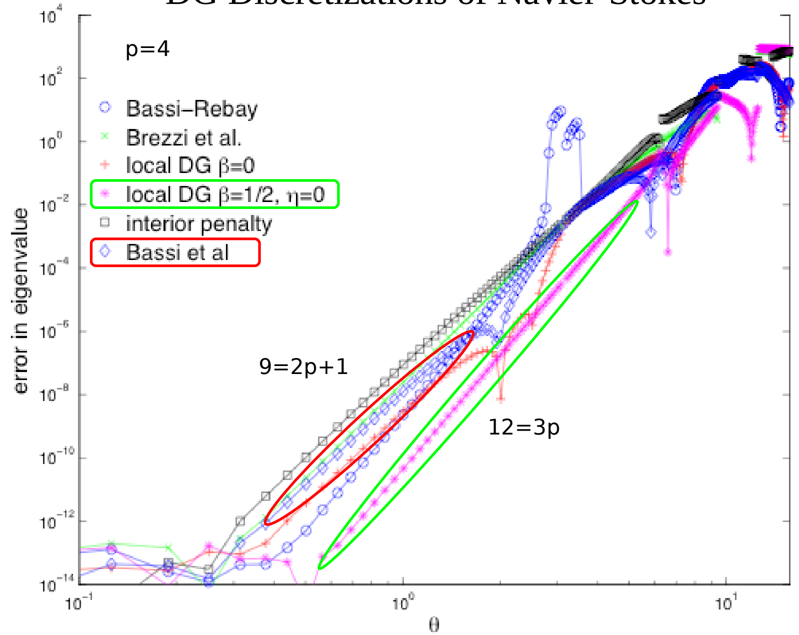

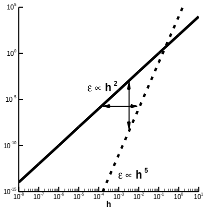

The Paradox of Super-Convergence

$$\mathbf{u}_h^n(\xi, t) = e^{-i\omega t}\lambda^n P_h(\xi)$$

eigenvalue is
super-convergent

- wavelength
- propagation speed
- growth/decay

...

eigenfunction is <u>not</u>
super-convergent

- instantaneous point values
- precise mode shape

...

Naturally occurring features

Vortex shedding from a viscous cylinder
Mach = 0.2, Re_d=200

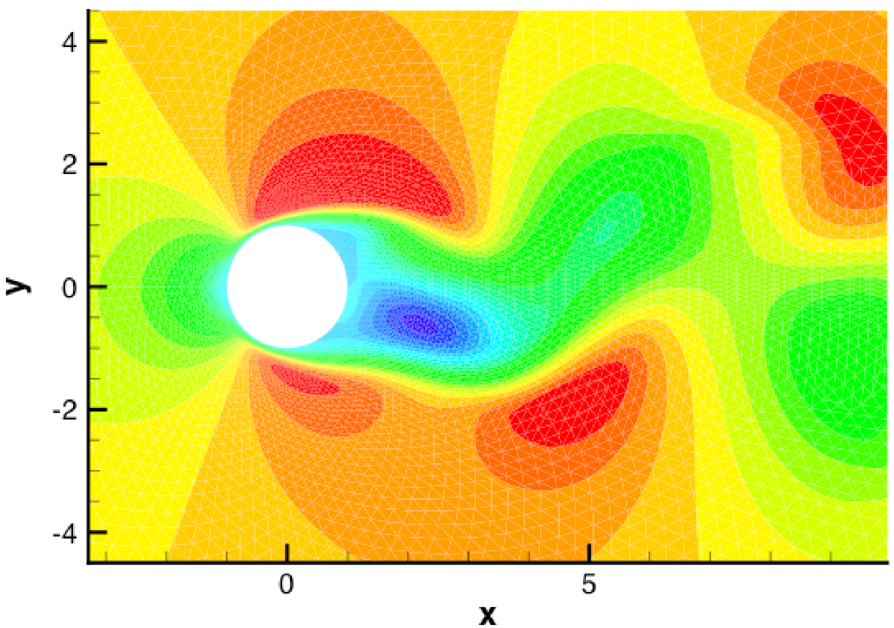

Convergence of period

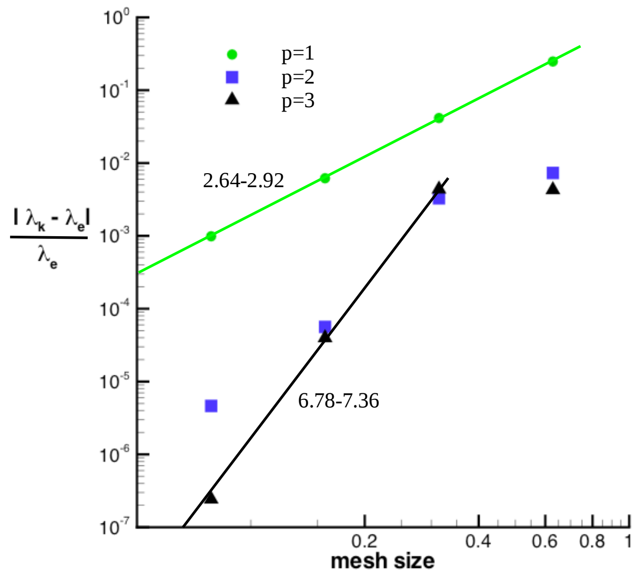

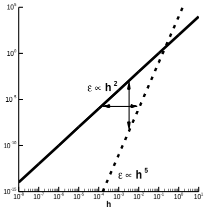

Solvers:
Challenges of DG for Navier Stokes

Explicit Eigenvalues

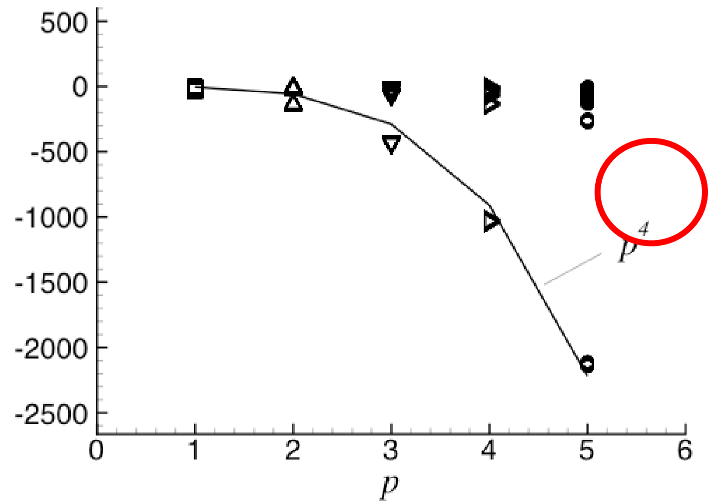

dt ∝ h^2/|max eigenvalue|

Stiffness ≈ |(max eigenvalue)/(min eigenvalue)|

h-multigrid, block relaxation

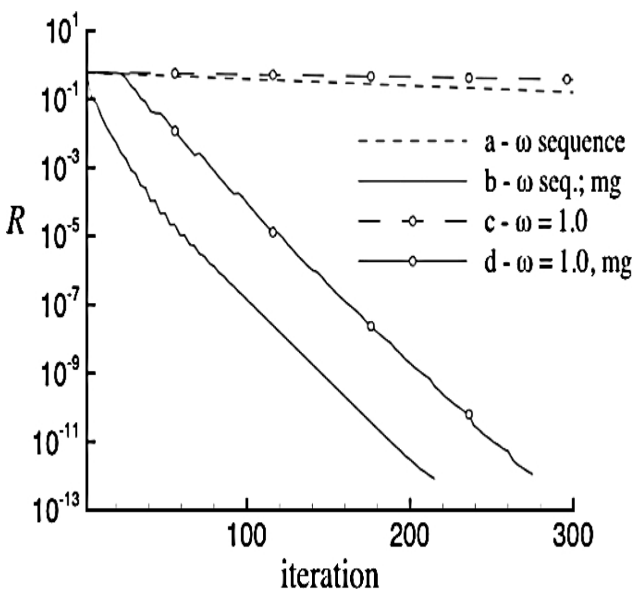

Theoretically possible...
but implementation on unstructured grids is difficult.

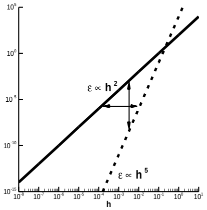

P-multigrid Solution Method

h-Multigrid

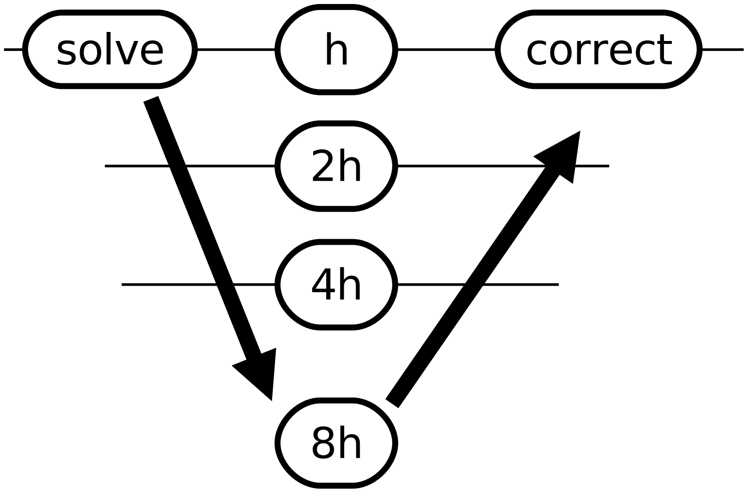

P- Multigrid

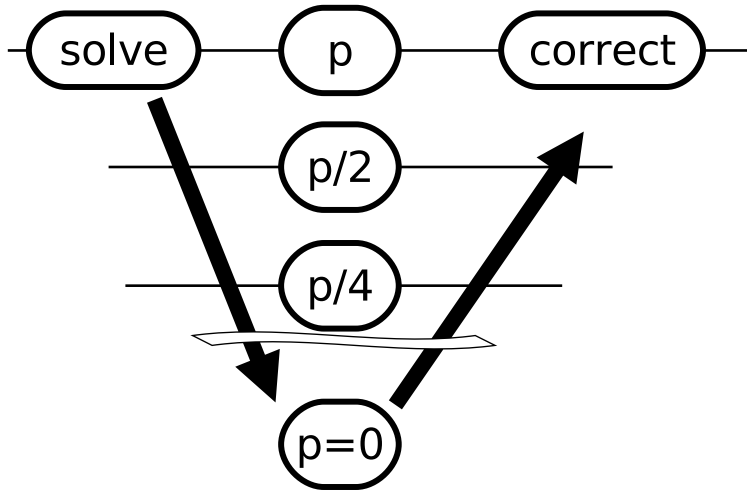

Each Coarsening:
- reduces number of unknowns
- reduces stiffness

Both contributions are critical

At the p=0 level, apply:
- h-multigrid
- GMRES
- direct solver
- relaxation

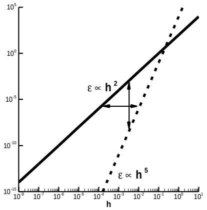

Analysis of restriction to p=0

Convergence Analysis:
2-level Versus Multi-level to p=0

p	Jacobi		Gauss-Seidel	
	2-level	multi-level	2-level	multi-level
1	0.70	0.70	0.80	0.80
2	0.27	0.98	0.17	0.90
4	0.52	0.89	0.33	0.95
8	0.80	1.00	0.67	0.98

0.14

0.43

p=0 discontinuous basis

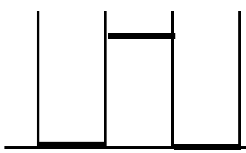

p=1 continuous basis

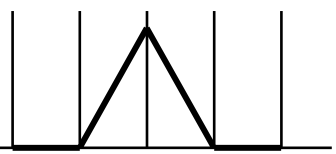

Eigenfunctions of DG applied to diffusion for p=1

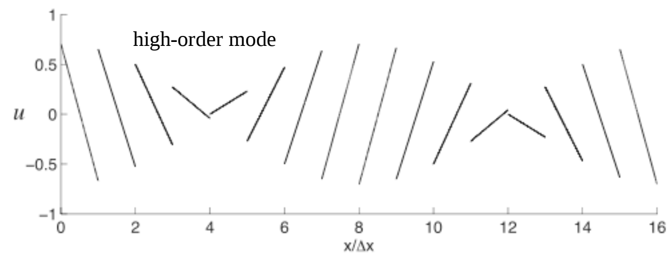

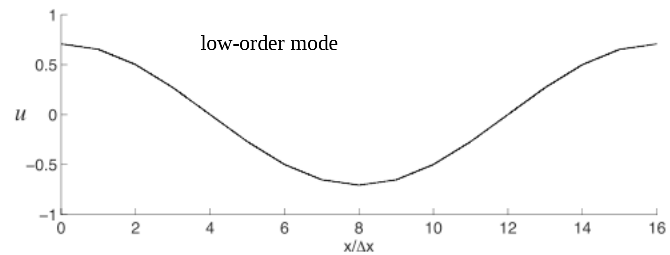

P=0 (piecewise constant) **cannot**:
- represent either mode.
- provide a correction.

P=1-continuous **can**:
- resolve and correct the low-order mode
- provide reduction in number of variables

P-multigrid: Analysis of DG applied to diffusion

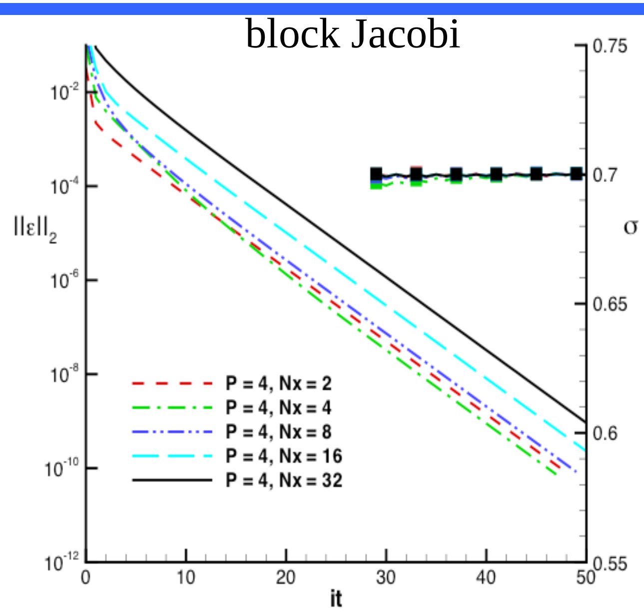

(a)

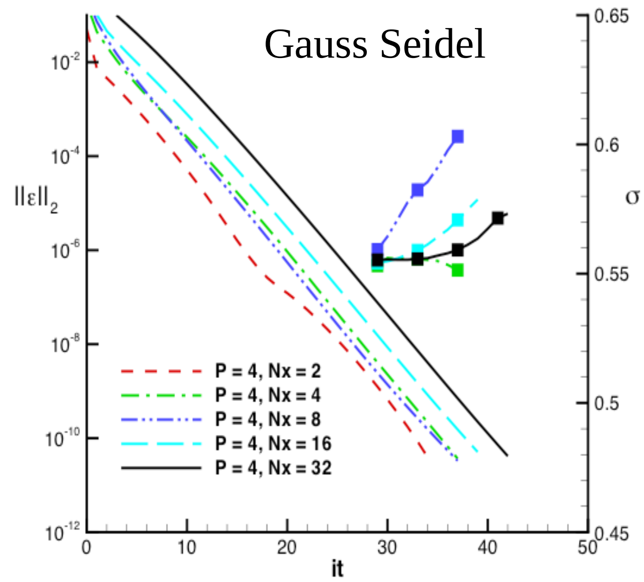

(b)

Mesh independent convergence (the holy grail!),
but with two caveats:

1. Careful construction of low-P equations.
2. Stop decent before P=0 -> restrict to P=1 continuous

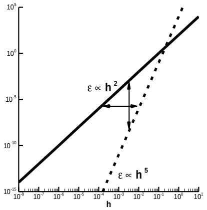

Conclusions for DG

- Rigorous analysis of DG's accuracy properties:
  - insensitive to mesh smoothness,
  - proofs of super-convergence,
  - insight into nature of DG's super-convergence properties.
- Uncovered and remedied several hidden flaws in P-multigrid:
  - requires careful construction of low-order equations,
  - restriction to p=1 continuous basis instead of p=0 discontinuous.

Careful analysis has helped to uncover and resolve several potential pitfalls, and has greatly improved our understanding of the strengths and limitations of the DG method.

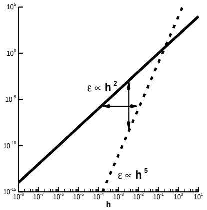

Outline

- Why High-Order / History / Impediments
- “Current” Langley Activity
  – Discontinuous Galerkin (Harold Atkins)
  – Energy Stable WENO
- Questions

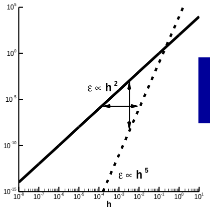

Boundary Closures for ESWENO Schemes

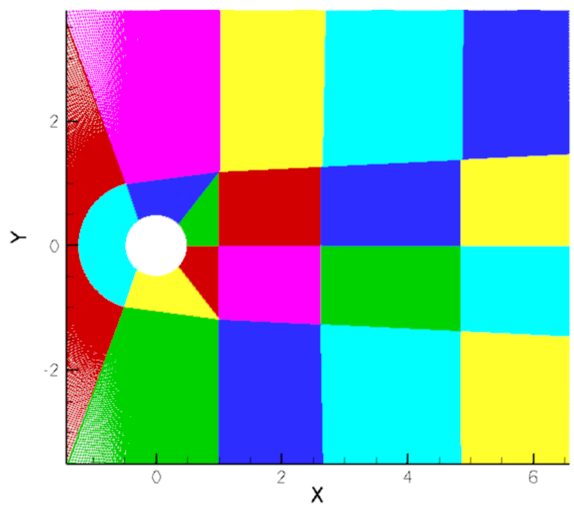

Travis Fisher (Purdue University)

Nail K. Yamaleev *(North Carolina A&T State University)*

Mark H. Carpenter *(NASA Langley Research Center)*

Applications with Shocks

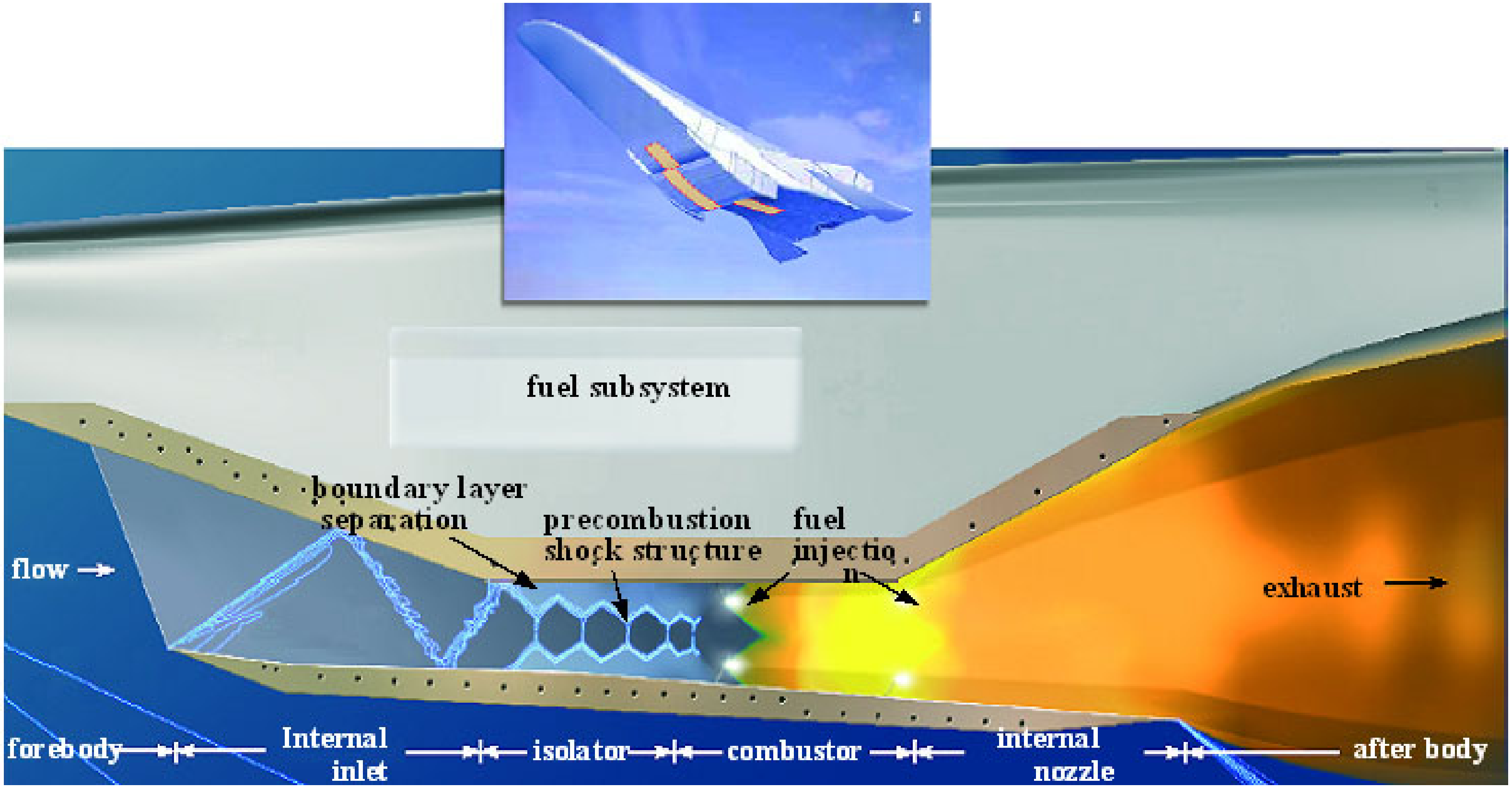

Hypersonic/Supersonic/Subsonic (Combustion, Shock BL interaction, BL stability, transition, turbulence,. . .)

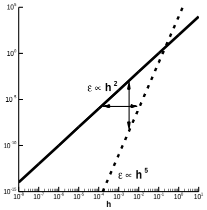

Big Picture: Complex Geometries

What's the plan?

- HOFD for Complex Geometries: Summation-by-parts HOFD (SBP)
  - High-Order Block Structured Finite-Difference: JCP 111(2), pp 220, 1994. (SSH 98)
  - Multi-Domain HO FD: JCP 148(2), pp. 341, 1999. (SSH 54)
    - Only C_0 Block Interface Connectivity: Geometric Flexibility
    - Penalty Interface Coupling between Blocks (SAT)
    - SBP-SAT: Design Order Accurate, L_2-Stability, Conservation
- Plan of Attack: Four Development Phases for ESWENO
  - Stability of WENO schemes on 1D periodic Domains (ESWENO): JCP 228(11), pp. 4248, 2009. (SSH 1)
  - Stability of Boundary Closure Operators
    - 4th-Order Central: NASA/TM-2009-216166
    - 6th-order/8th-order central
  - Stability of discontinuity crossing interface
  - Nonlinear Stability proofs

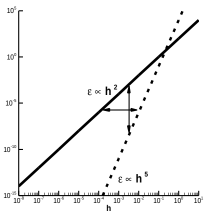

6th-order WENO Schemes:

$$U_t + F_x = 0$$

$$\frac{du_j}{dt} + \frac{f^W_{j+1/2} - f^W_{j-1/2}}{\Delta x} = 0$$

The 6th-order WENO flux

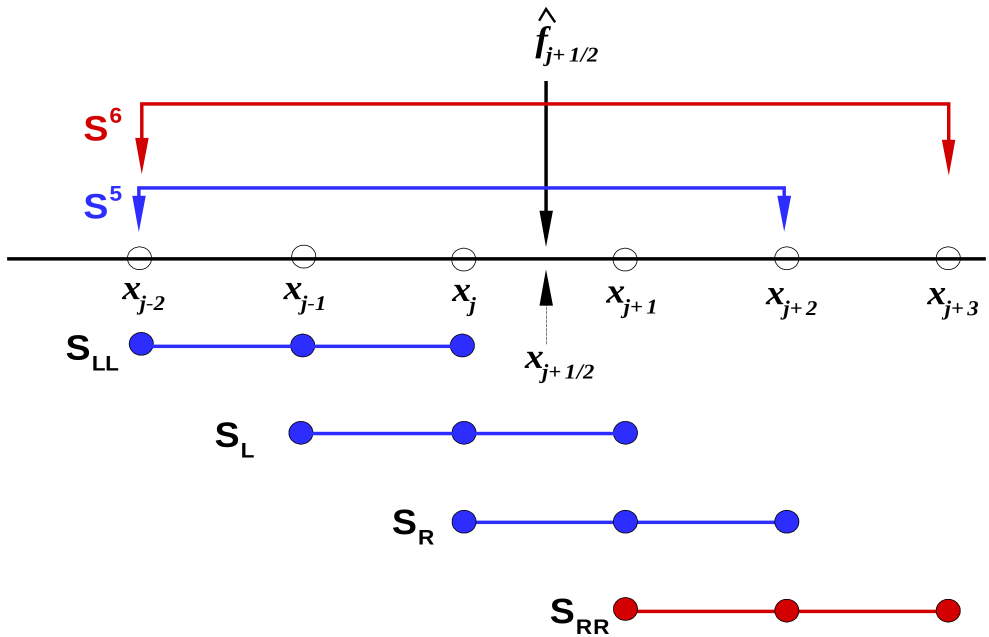

$$f^W_{j+1/2} = \omega^{LL}_{j+1/2} f^{LL}_{j+1/2} + \omega^{L}_{j+1/2} f^{L}_{j+1/2} + \omega^{R}_{j+1/2} f^{R}_{j+1/2} + \omega^{RR}_{j+1/2} f^{RR}_{j+1/2}$$

$$\begin{bmatrix} f^{LL}_{j+1/2} \\ f^{LL}_{j+1/2} \\ f^{LL}_{j+1/2} \\ f^{LL}_{j+1/2} \end{bmatrix} = \frac{1}{6}\begin{pmatrix} 2 & -7 & 11 & & & 0 \\ & -1 & 5 & 2 & & \\ & & 2 & 5 & -1 & \\ 0 & & & 11 & -7 & 2 \end{pmatrix}\begin{bmatrix} f_{j-2} \\ f_{j-1} \\ f_j \\ f_{j+1} \\ f_{j+1} \\ f_{j+1} \end{bmatrix}$$

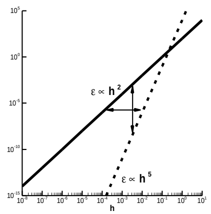

6th-order WENO Schemes

The weights should satisfy the following properties:

$$0 \le \omega_{j+1/2}^{r} \le 1, \quad \sum_{r} \omega_{j+1/2}^{r} = 1, \quad \forall j$$

$$\omega_{j+1/2}^{r} = d_r + O(\Delta x^{p-s+1})$$

Conventional weights of Jiang and Shu:

$$\omega_{j+1/2}^{r} = \frac{\alpha_r}{\sum_{l} \alpha_l}, \quad \alpha_r = \frac{d_r}{\left(\varepsilon + \beta_r\right)^2}, \quad \beta_r = \sum_{k=1}^{s-1} \Delta x^{2k-1} \int_{x_{j-1/2}}^{x_{j+1/2}} \left(\frac{d^k q_r(x)}{dx^k} \right)^2 dx \Rightarrow \omega^r = d^r + O(\Delta x^2)$$

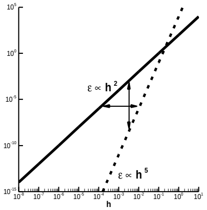

Useful References

ENO/WENO SCHEMES

- A. Harten, B. Engquist, S. Osher, and S. Chakravarthy

  "Uniformly high order essentially non-oscillatory schemes, III," *J. of Computational Physics*, Vol. 71, pp. 231-303, 1987.

  – Adaptively chooses "smoothest" stencil from *s* candidates. Provides s^{th}-order accuracy.

- X.-D. Liu, S. Osher, and T. Chan

  "Weighted Essentially Non-oscillatory Schemes," *J. of Computational Physics*, Vol. 115, pp. 200-212, (1994).

  – Uses a weighted convex combination of all *s* candidate stencils. Provides $(s+1)^{th}$-order accuracy.

- G. Jiang and C.-W. Shu

  "Efficient implementation of weighted ENO schemes," *J. of Computational Physics*, Vol. 126, pp. 202-228, (1996). (SSH 698)

  – Generalization to the FD formulation. Provides $(2s-1)^{th}$-order accuracy on sufficiently fine meshes.

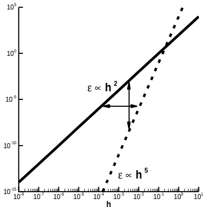

Remaining Issues: Accuracy

Left Achilles Heel of High-Order WENO Schemes

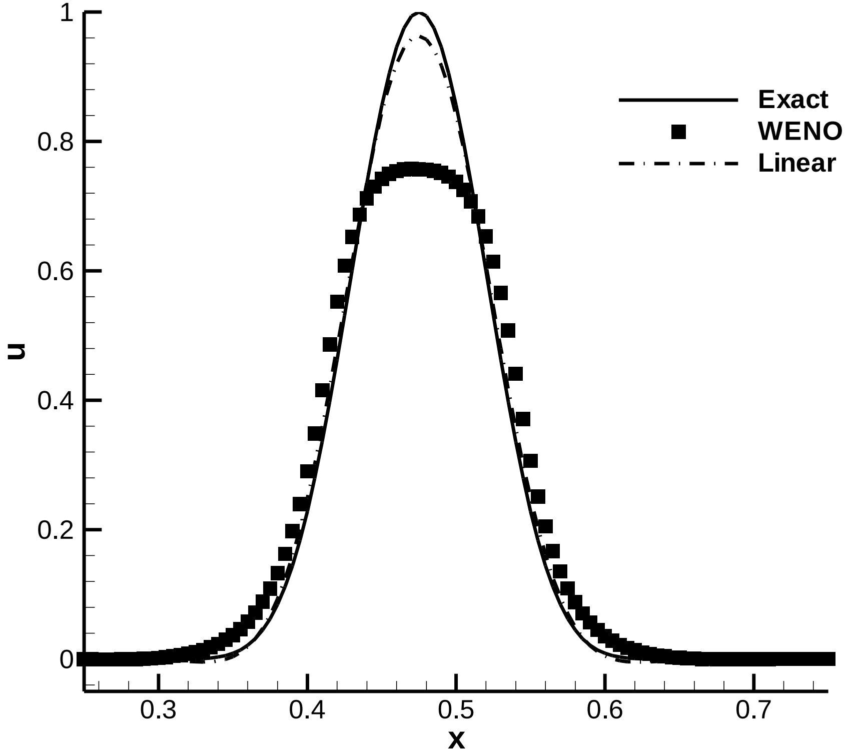

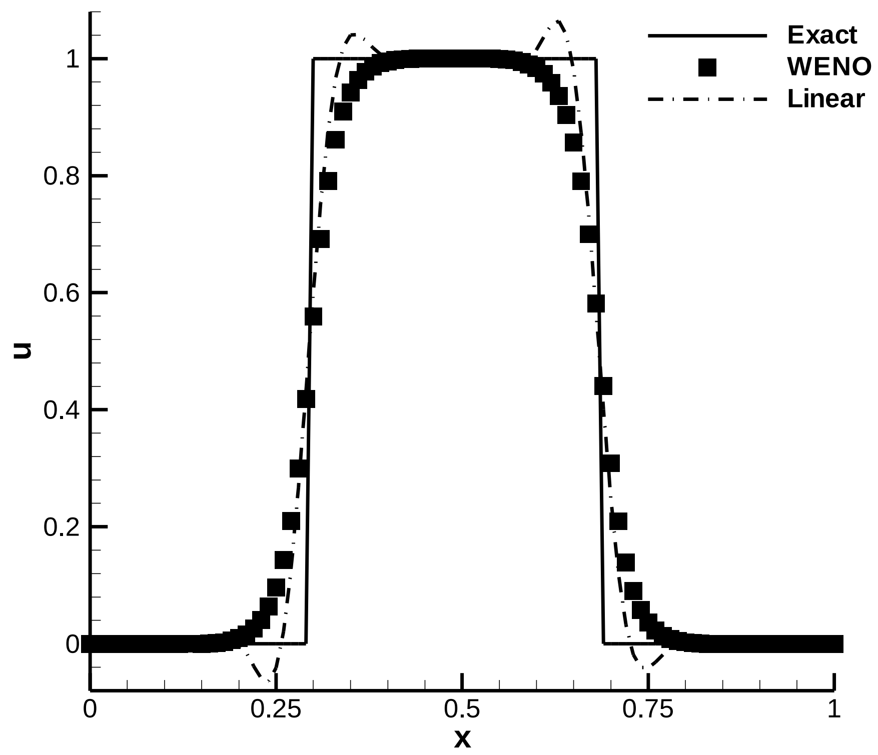

Moving pulse simulation using the 3rd-order WENO scheme

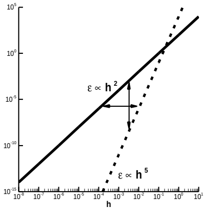

Remaining Issues: Boundaries

Right Achilles Heel of High-Order WENO Schemes

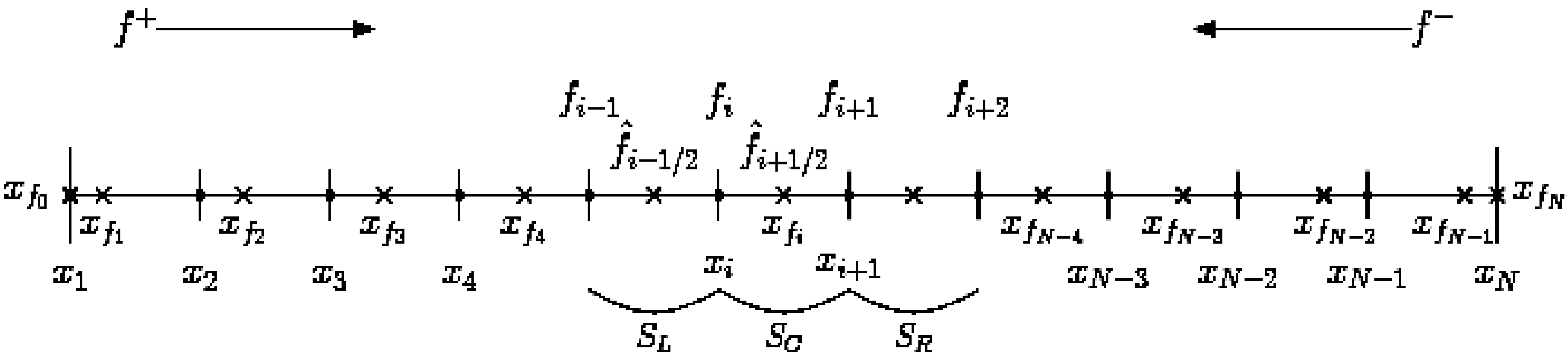

Grabbing data outside the domain: 4th-order WENO scheme

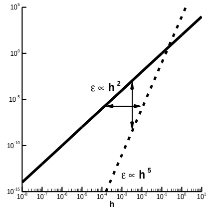

Needed Improvements for WENO

- **Improvements needed by conventional WENO:**
  - The WENO schemes are too dissipative as compared with the corresponding target linear schemes
    - Typically based on upwind operators.
    - The order of the conventional WENO schemes deteriorates from $(2s-1)$ to s at critical points.
  - For some steady state problems, the residual cannot be driven to the machine zero.
  - No stability proofs are available for discontinuous solutions of hyperbolic systems.
  - Boundary stencils and extension to complex geometry

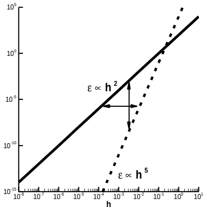

Energy Stable WENO

Accomplishments to date (ROYOT)

- *Energy Stable* WENO (ESWENO)
  - A WENO-type scheme that is stable in the L_2 norm by construction for **continuous and discontinuous solutions**
- Developed New weights
  - Faster convergence to the underlying linear scheme
  - Improved shock-capturing capabilities
- Boundary Closures for 4th-order ESWENO
  - Design order accurate (3-4-3)

    Full stencil biasing up to boundaries (almost)

    L_2 Stability
- Maintains original properties
  - Design order of accuracy for smooth solutions/extrema
  - Conservative (Lax-Wendroff theorem)
  - Essentially nonoscillatory solutions

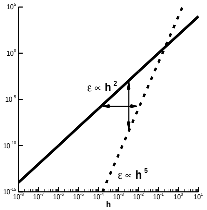

Energy Estimates

Continuous problem

$$\frac{\partial u}{\partial t}+\frac{\partial f}{\partial x}=\sum_{n=1}^{N}(-1)^{n-1}\frac{\partial^n}{\partial x^n}\left(\mu_n(u)\frac{\partial^n u}{\partial x^n}\right)\quad f=au,\quad a>0,\quad \mu_n\geq 0 \quad (1)$$

Multiplying Eq. (1) by *u* and integrating over [0,1] yields

$$\frac{1}{2}\frac{d}{dt}\|u\|_{l_2}^2+\frac{1}{2}au^2\Big|_0^1=\sum_{n=1}^{N}\int_0^1(-1)^{n-1}u\frac{\partial^n}{\partial x^n}\left(\mu_n(u)\frac{\partial^n u}{\partial x^n}\right)dx$$

Integrating RHS by parts yields

$$\frac{d}{dt}\|u\|_{l_2}^2 + a\,u^2\Big|_0^1 = -2\sum_{n=1}^{N}\int_0^1\mu(u)\left(\frac{\partial^n u}{\partial x^n}\right)^2 dx \leq 0$$

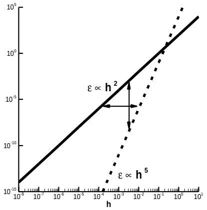

Energy Estimates (cont.)

Discrete problem

$$\frac{\partial \mathbf{u}}{\partial t} + P^{-1} Q \mathbf{f} = -\sum_{n=0}^{S} P^{-1} D_1^n \Lambda_n [D_1^n]^T \mathbf{f} \qquad (2)$$

Multiplying Eq. (2) by $\mathbf{u}^T P$ and adding it to its transpose yields

$$\frac{d}{dt}\|u\|_P^2 + a\mathbf{u}^T\left(Q + Q^T\right)\mathbf{u} = -a\sum_{n=0}^{S}\left([D_1^n]^T\mathbf{u}\right)^T\left(\Lambda_n + \Lambda_n^T\right)D_1^n]^T\mathbf{u}$$

What if:

$$P = P^T \; ; \; \psi^T P \psi > 0 \; ; \; Q + Q^T = Diag[-1,0,\cdots,0,1] \; ; \; \psi^T\left(\Lambda + \Lambda^T\right)\psi \geq 0$$

$$\frac{\partial f}{\partial x} = P^{-1} Q \boldsymbol{f} + \sum_{n=0}^{S} P^{-1} D_1^n \Lambda_n [D_1^n]^T \boldsymbol{f} + O\left(\Delta x\right)^{2s}$$

Then

$$\frac{d}{dt}\|\boldsymbol{u}\|_P^2 + a\,\boldsymbol{u}^2\Big|_0^1 = -2\sum_{n=0}^{N}\left([D_1^n]^T\boldsymbol{u}\right)^T \Lambda_n\left([D_1^n]^T\boldsymbol{u}\right) \leq 0$$

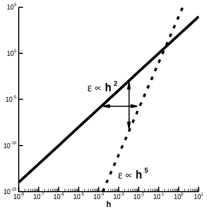

6th-order WENO Schemes: Are They Stable?

Can WENO schemes be represented as $\frac{\partial \mathbf{u}}{\partial t} + P^{-1}Q\mathbf{f} = -\sum_{n=0}^{S} P^{-1} D_1^n \Lambda_n [D_1^n]^T \mathbf{f}$?

The 6th-order WENO operator: $[D_W \mathbf{f}]_j = \dfrac{f^W_{j+1/2} - f^W_{j-1/2}}{\Delta x}$

$$D_W = \frac{1}{2}\left(D_W - D_W^T\right) + \frac{1}{2}\left(D_W + D_W^T\right) = P^{-1}Q + P^{-1}D_W^{sym}$$

Is D_W^{sym} Stable? Find a constructive stability test????

$$D_W^{sym} = P^{-1} M (A + A^T) M^T$$

$$D_W^{sym} = P^{-1}\left(D_1^3 \Lambda_3^W [D_1^3]^T + D_1^2 \Lambda_2^W [D_1^2]^T + D_1^1 \Lambda_1^W [D_1^1]^T + D_1^0 \Lambda_0^W [D_0^3]^T\right)$$

$$\Lambda_3^W = \frac{1}{6} diag\left[\omega^{LL}_{j+5/2} - \omega^{RR}_{j+5/2}\right]$$

$$\Lambda_2^W = \frac{1}{12} diag\left[\omega^{LL}_{j+3/2} - 4\omega^{LL}_{j+5/2} + \omega^{L}_{j+3/2} - \omega^{R}_{j+1/2} + 4\omega^{RR}_{j-1/2} - \omega^{RR}_{j+1/2}\right]$$

$$\Lambda_1^W = \frac{1}{12} diag\left[3\omega^{LL}_{j+1/2} - 5\omega^{LL}_{j+3/2} + 2\omega^{LL}_{j+5/2} + \omega^{L}_{j+1/2} - \omega^{L}_{j+3/2} + \omega^{R}_{j-1/2} - \omega^{R}_{j+1/2} - 2\omega^{RR}_{j-3/2} + 5\omega^{RR}_{j-1/2} - 3\omega^{RR}_{j+1/2}\right]$$

$$\Lambda_0^W = \frac{1}{2} diag\left[-\omega^{LL}_{j-1/2} - \omega^{L}_{j-1/2} - \omega^{R}_{j-1/2} - \omega^{RR}_{j-1/2} + \omega^{LL}_{j+1/2} + \omega^{L}_{j+1/2} + \omega^{R}_{j+1/2} + \omega^{RR}_{j+1/2}\right] = 0$$

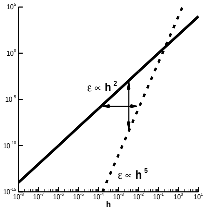

6th-order WENO Schemes

Conventional WENO schemes:

- No energy estimate/stability proof (that we could find)
- The WENO dissipation operator is **not positive semi-definite**, because for unresolved solutions $\Lambda_n^W < 0, n = \overline{1,3}$!
- For discontinuous or unresolved solutions, the WENO artificial dissipation operator $-P^{-1}\sum_{n=1}^{3} D_1^n \Lambda_n^W [D_1^n]^T$ could have positive eigenvalues, thus indicating that the scheme may become locally unstable.

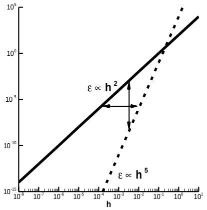

6th-order ESWENO Schemes

Stability

ESWENO scheme has ***all the terms*** of the 6th-order WENO scheme and also includes ***an additional artificial dissipation term***

$$\frac{\partial \mathbf{u}}{\partial t} + P^{-1} Q \mathbf{f} = -\sum_{n=0}^{3} P^{-1} D_1^n \Lambda_n^{ES} [D_1^n]^T \mathbf{f}$$

Central operator: $P = \Delta x I, \quad Q = P D_W^{skew}$

Additional artificial dissipation operator: $\overline{D}_{ad} = -P^{-1} \sum_{n=1}^{3} D_1^n \overline{\Lambda}_n [D_1^n]^T$

$$\left(\overline{\lambda}_n\right)_{j,j} = \frac{1}{2}\left[\sqrt{\left(\lambda_n^W\right)_{j,j}^2 + \delta_n^2} - \left(\lambda_n^W\right)_{j,j}\right]$$

$$D^{ES} = D^W + \overline{D}_{ad}$$

$$\left(\lambda_n^{ES}\right)_{j,j} = \left(\lambda_n^W\right)_{j,j} + \left(\overline{\lambda}_n\right)_{j,j} = \frac{1}{2}\left[\sqrt{\left(\lambda_n^W\right)_{j,j}^2 + \delta_n^2} + \left(\lambda_n^W\right)_{j,j}\right] > 0 \text{ for any } u_j \text{ and } \forall j$$

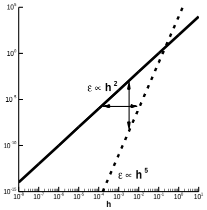

6th-order ESWENO Schemes

The weights should satisfy the following properties:

$$0 \le \omega^r_{j+1/2} \le 1, \quad \sum_r \omega^r_{j+1/2} = 1, \quad \forall j$$

$$\omega^r_{j+1/2} = d_r + O(\Delta x^{p-s+1})$$

Conventional weights of Jiang and Shu:

$$\omega^r_{j+1/2} = \frac{\alpha_r}{\sum_l \alpha_l}, \quad \alpha_r = \frac{d_r}{(\varepsilon + \beta_r)^2}, \quad \beta_r = \sum_{k=1}^{s-1} \Delta x^{2k-1} \int_{x_{j-1/2}}^{x_{j+1/2}} \left(\frac{d^k q_r(x)}{dx^k} \right)^2 dx \Rightarrow \omega^r = d^r + O(\Delta x^2)$$

<u>New weights with Smooth Consistency</u>

$$\omega^r_{j+1/2} = \frac{\alpha_r}{\sum_k \alpha_k}, \quad \alpha_r = d_r \left(1 + \frac{\tau_5}{\varepsilon + \beta_r} \right), \quad r = \{LL, L, R, RR\}$$

$$\tau_5 = \begin{cases} \left(-f_{j-2} + 5 f_{j-1} - 10 f_j + 10 f_{j+1} - 5 f_{j+2} + f_{j+3} \right)^2, \ \text{for } \varphi \ne 0 & \Rightarrow \quad \omega^r = d^r + O(\Delta x^8) \\ \left(f_{j-2} - 4 f_{j-1} + 6 f_j - 4 f_{j+1} + f_{j+2} \right)^2, \ \text{for } \varphi = 0 & \Rightarrow \quad \omega^r = d^r + O(\Delta x^6) \end{cases}$$

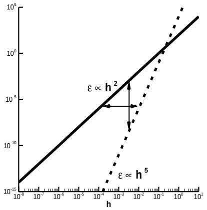

Numerical Results

Linear Wave Equation

The 5th- and 6th-order WENO and ESWENO schemes (Gaussian pulse)

L_∞ error norm

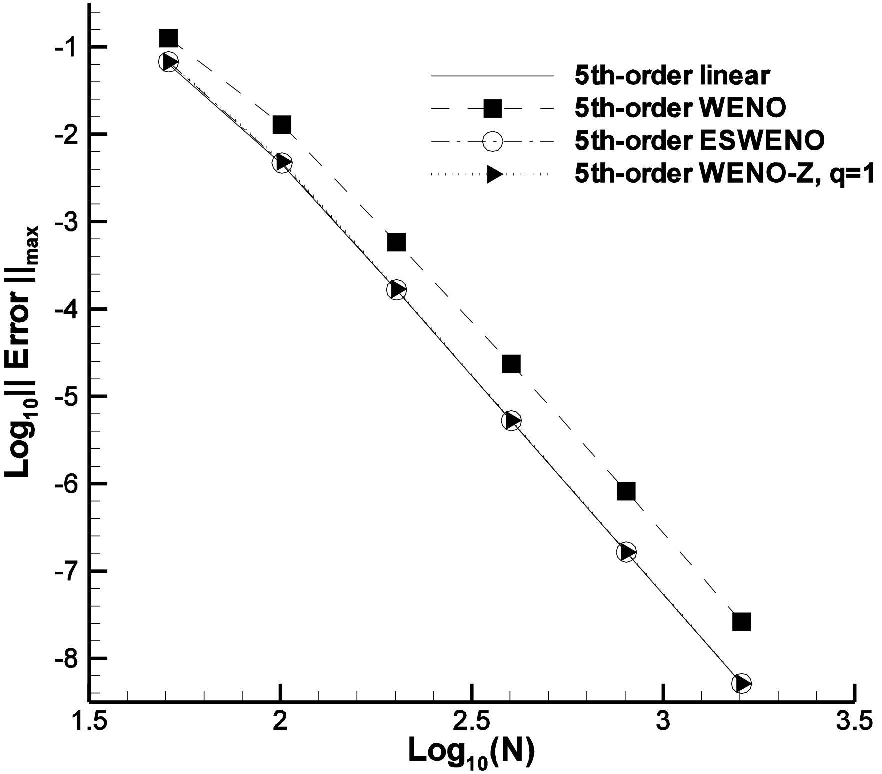

L_∞ error norm

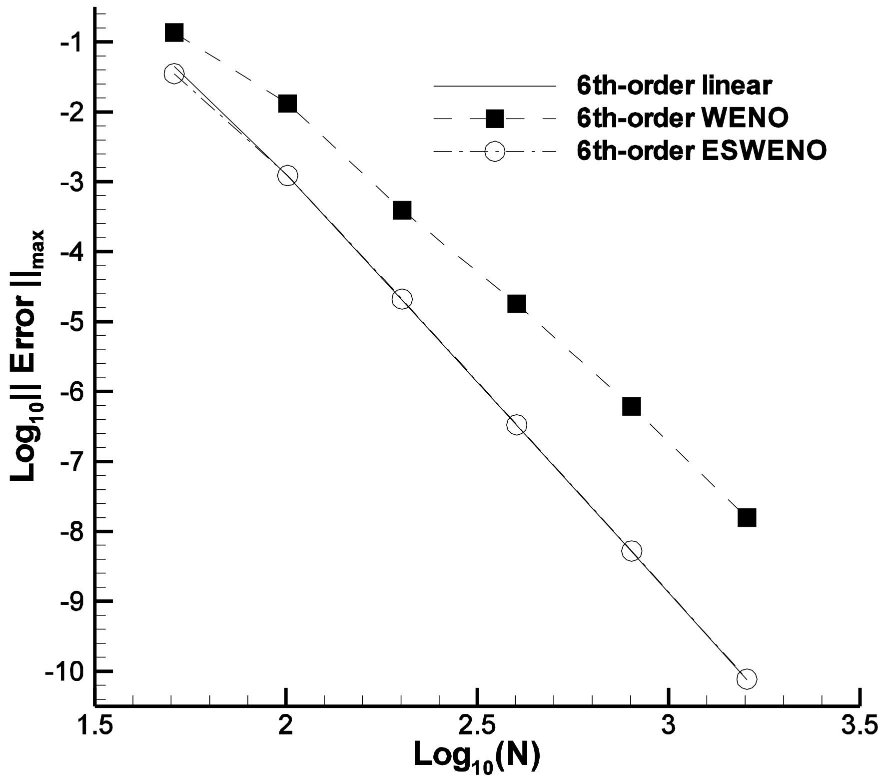

4th-order WENO Schemes

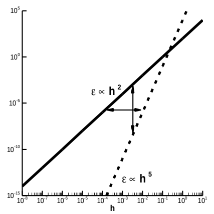

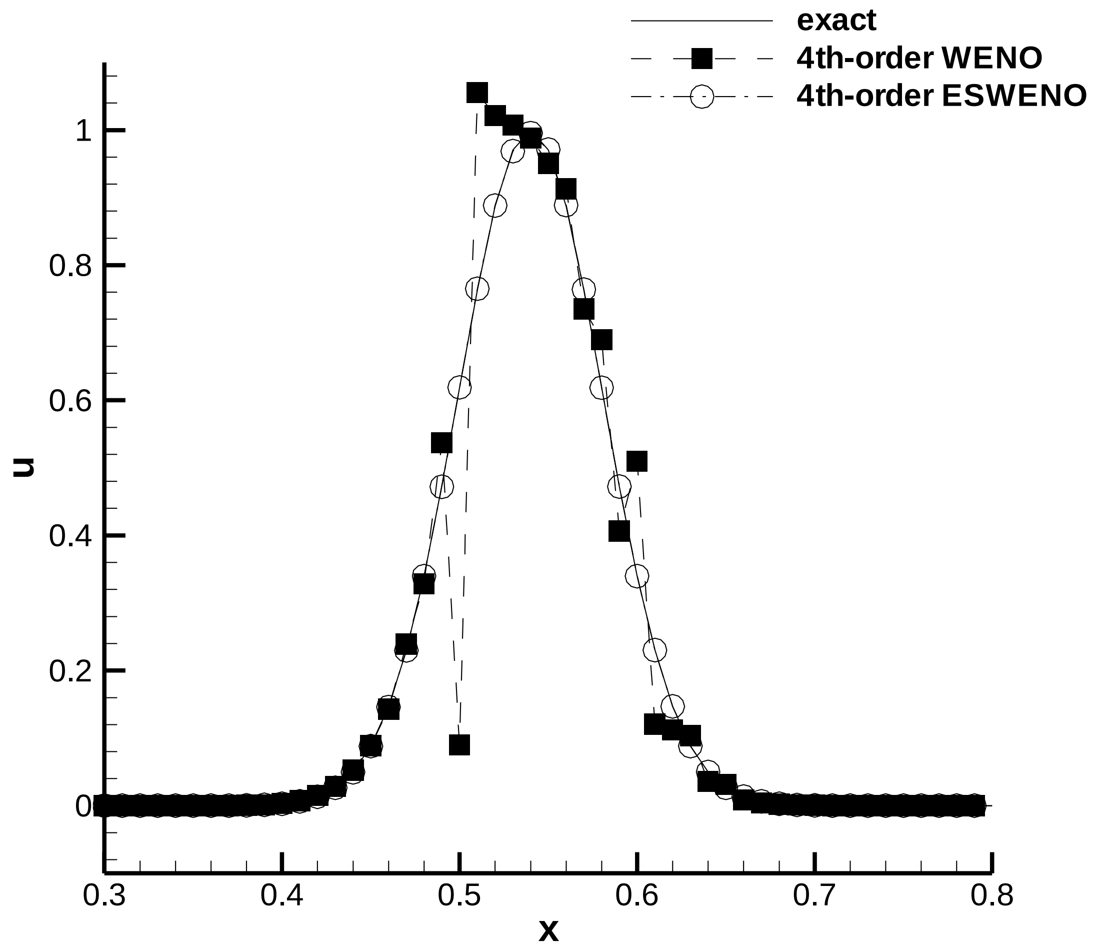

Solution obtained with the 4th-order WENO scheme for the linear wave equation with initial condition $u_0(x) = e^{-300(x-0.5)^2}$.

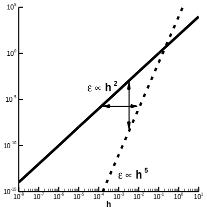

Numerical Results (cont.)

Linear Wave Equation

The 5th-order WENO and ESWENO schemes (solution with critical points)

L_∞ error norm

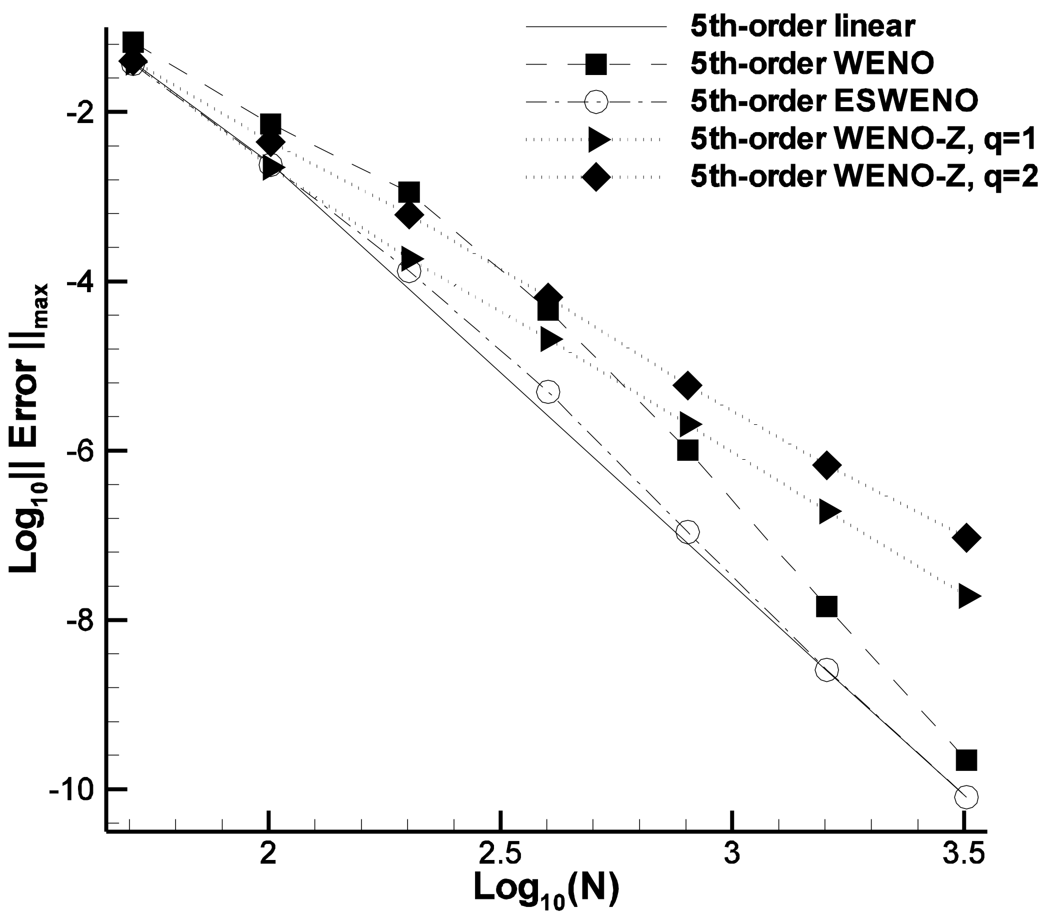

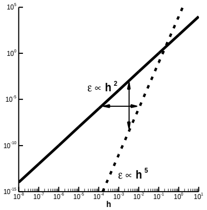

Numerical Results (cont.)

Steady Quasi-1-D Euler Equations

The

Quasi-1-D nozzle problem, 5th and 6th-order WENO and ESWENO schemes (Mach=1.5, *J*=51 grid points)

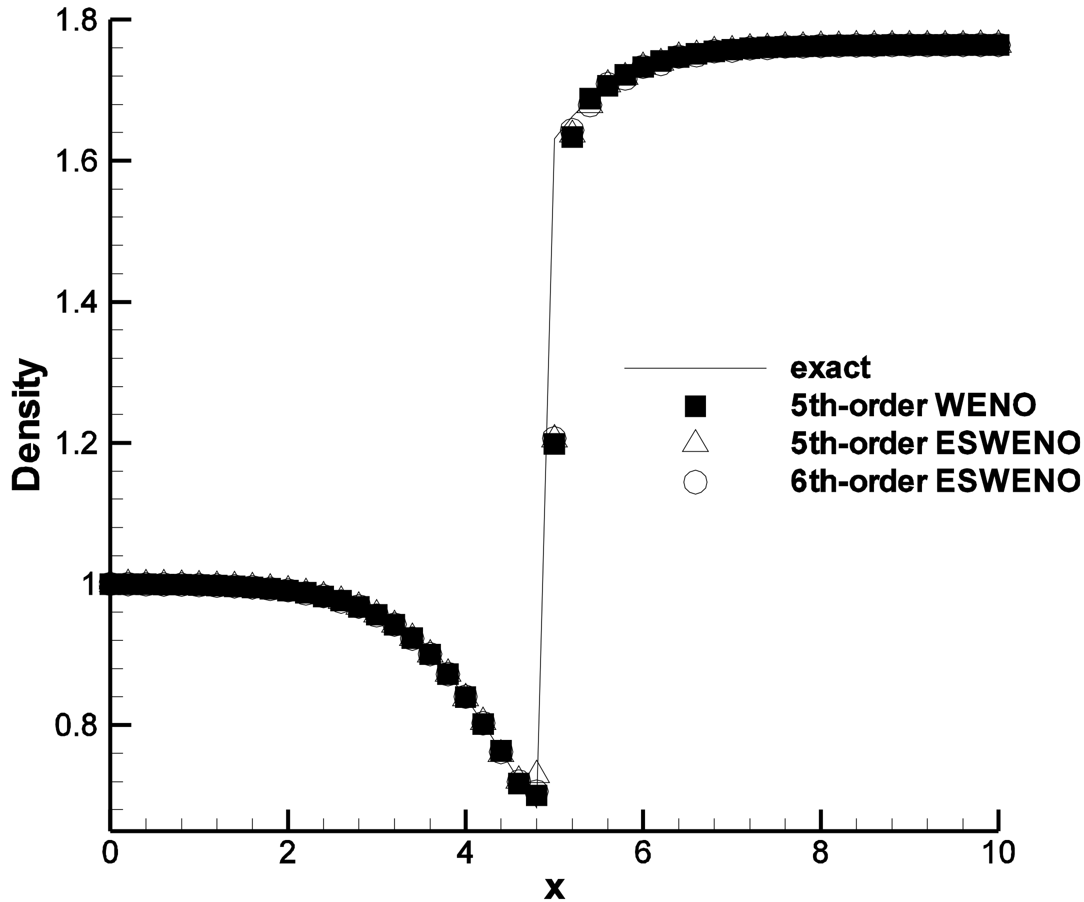

Numerical Results (cont.)

Unsteady 1-D Euler Equations

Shock/acoustic wave interaction problem , 5th and 6th-order WENO and ESWENO schemes (*J*=300 grid cells)

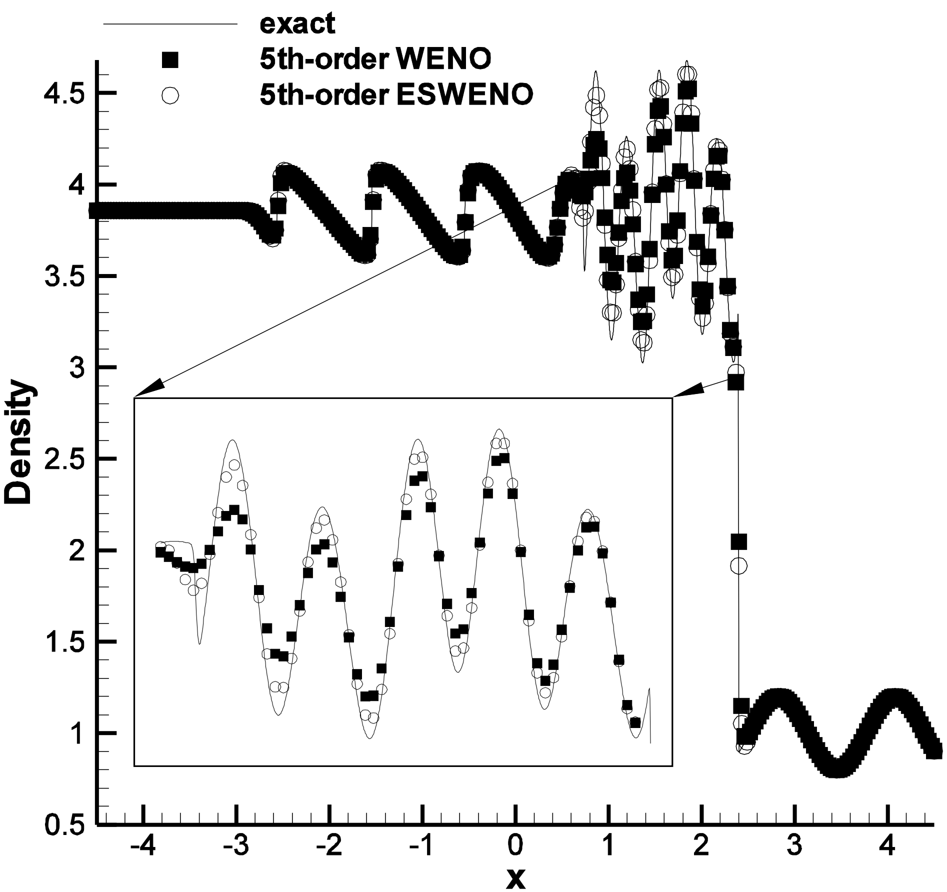

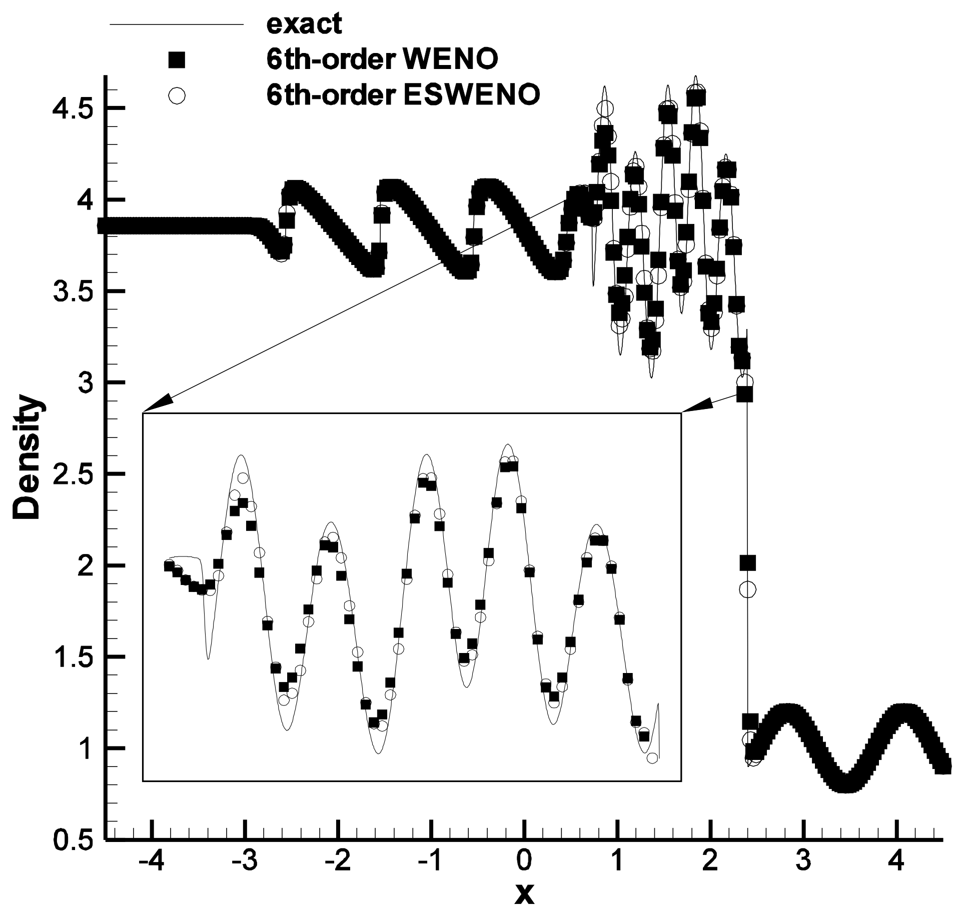

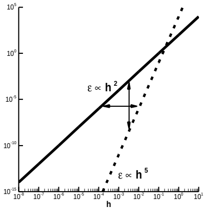

Boundary Closures: The Plan?

- **Goals**
  - **Conventional WENO stencil biasing to boundary**
    - **4th-order: only volume next to wall has reduced bias**
  - **Use Centered SBP scheme as WENO target operator**
    - **Resolved flow then operator reduces to SBP operator**
    - **Prove stability/accuracy of target operator**
- **Plan**
  - **Derive general "4th-order" SBP discrete matrix (with BCs)**
  - **Express WENO stencil biasing mechanics in matrix form**
  - **Equate the two forms (matrices) and see what happens**

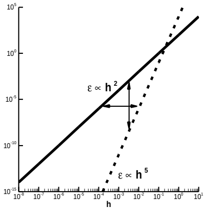

Boundary Closures: The Plan
Summation-By-Parts (3-4-3)

- **Boundary stencils of $O(\Delta x^{p-1}) \Rightarrow O(\Delta x^{p})$ Global accuracy**
  - **B. Gustafsson, Math. Comp. 29, 130, 1975**
- **Summation-by-parts operators**
  - **H.-O. Kreiss, G. Scherer, Math. Aspects FE PDEs 1974**
  - **B. Strand, J. Comp. Phy., 110, 1, 1994. For example**

$$D = P^{-1}Q \;;\; P = P^{T} \;;\; \psi^{T} P \psi > 0 \;;\; Q + Q^{T} = Diag[-1,0,\cdots,0,1] \;;$$

$$P = \begin{pmatrix} \frac{1}{4} & \frac{19}{144} & \frac{-11}{216} & \frac{-7}{216} & 0 & 0 \\ \frac{19}{144} & \frac{65}{54} & \frac{5}{108} & \frac{23}{216} & 0 & 0 \\ \frac{-11}{216} & \frac{5}{108} & \frac{91}{108} & \frac{-7}{432} & 0 & 0 \\ \frac{-7}{216} & \frac{23}{216} & \frac{-7}{432} & \frac{55}{54} & 0 & 0 \\ 0 & 0 & 0 & 0 & 1 & 0 \\ 0 & 0 & 0 & 0 & 0 & 1 \end{pmatrix} \;;\quad Q = \begin{pmatrix} \frac{-1}{2} & \frac{593}{864} & \frac{-37}{216} & \frac{-13}{864} & 0 & 0 \\ \frac{-593}{864} & 0 & \frac{191}{288} & \frac{5}{216} & 0 & 0 \\ \frac{37}{216} & \frac{-191}{288} & 0 & \frac{497}{864} & \frac{-1}{12} & 0 \\ \frac{13}{864} & \frac{-5}{216} & \frac{-497}{864} & 0 & \frac{2}{3} & \frac{-1}{12} \\ 0 & 0 & \frac{1}{12} & \frac{-2}{3} & 0 & \frac{2}{3} \\ 0 & 0 & 0 & \frac{1}{12} & \frac{-2}{3} & 0 \end{pmatrix}$$

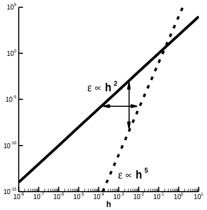

Boundary Closures: SBP (3-4-3) General Parameterization

- **Pentadiagonal 4th-order:** $Q_i = Pentadiagonal[\frac{1}{12}, \frac{-8}{12}, 0, \frac{8}{12}, \frac{-1}{12}];$

$$P = \Delta x \begin{pmatrix} P_0 & 0 & 0 \\ 0 & I & 0 \\ 0 & 0 & P_0^{PT} \end{pmatrix} \quad ; \quad Q = \begin{pmatrix} Q_0 & Q_d & 0 \\ -Q_d & Q_i & Q_d \\ 0 & -Q_d^{\,T} & -Q_0^{PT} \end{pmatrix}$$

$$P_0 = \begin{pmatrix} p_{11} & p_{12} & p_{13} & p_{14} \\ p_{12} & p_{22} & p_{23} & p_{24} \\ p_{13} & p_{23} & p_{33} & p_{34} \\ p_{14} & p_{24} & p_{34} & p_{44} \end{pmatrix} \; ; \; Q_0 = \begin{pmatrix} \frac{-1}{2} & q_{12} & q_{13} & q_{14} \\ q_{12} & 0 & p_{23} & q_{24} \\ q_{13} & q_{23} & 0 & q_{34} \\ q_{14} & q_{24} & q_{34} & 0 \end{pmatrix} \; ; \; Q_d = \begin{pmatrix} \cdots & 0 & 0 & 0 \\ 0 & \cdots & 0 & 0 \\ \frac{-1}{12} & 0 & \cdots & 0 \\ \frac{8}{12} & \frac{-1}{12} & 0 & \cdots \end{pmatrix} \; ;$$

- **General (3-4-3) two parameter solution after satisfying constraints on matrix properties and accuracy conditions**

$$D = P^{-1}Q \; ; \; P = P^T \; ; \; \psi^T P \psi > 0 \; ; \; Q + Q^T = Diag[-1, 0, \cdots, 0, 1] \; ;$$

$$P_{3-4-3} = P_{3-4-3}(\alpha_{1,} \alpha_2) \quad ; \quad Q_{3-4-3} = Q_{3-4-3}(\alpha_{1,} \alpha_2)$$

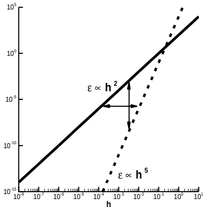

WENO Stencil Biasing Mechanics

$$U_t + F_x = 0$$

$$\frac{du_j(t)}{dt} + \frac{f^{ES}_{j+1/2} - f^{ES}_{j-1/2}}{\Delta x} = 0$$

- **Complementary Grids: Solution grid and Flux grid**

$$\boldsymbol{x}_N = \left[x_1, x_2, \cdots, x_{N-1}, x_N\right]^T \;;\; \bar{\boldsymbol{x}} = \left[\bar{x}_0, \bar{x}_1, \cdots, \bar{x}_{N-1}, \bar{x}_N\right]^T$$

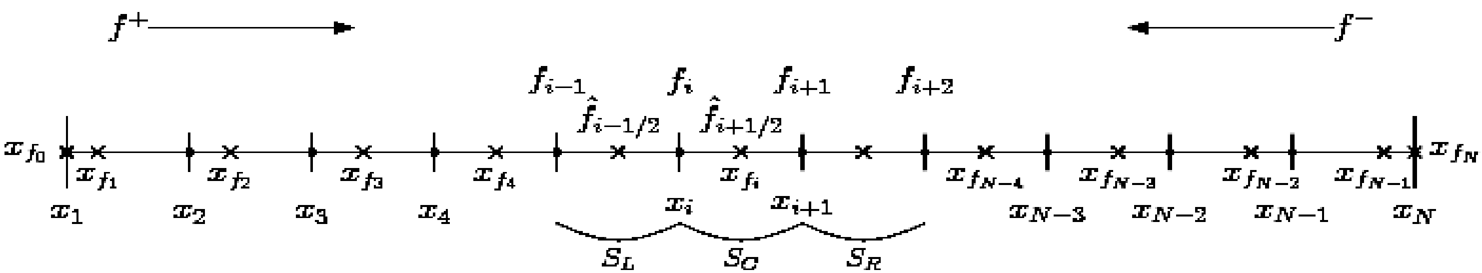

$$f^{ES}_{j+1/2} = \bar{\omega}^L_{j+1/2}\bar{f}^L_{J+1/2} + \bar{\omega}^C_{j+1/2}\bar{f}^C_{J+1/2} + \bar{\omega}^R_{j+1/2}\bar{f}^R_{J+1/2}$$

$$\bar{\boldsymbol{f}}^L = I^L_{fs}\boldsymbol{f} \;;\; \bar{\boldsymbol{f}}^C = I^C_{fs}\boldsymbol{f} \;;\; \bar{\boldsymbol{f}}^R = I^R_{fs}\boldsymbol{f}$$

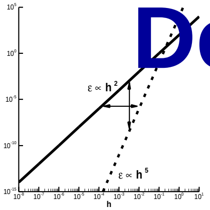

Deriving SBP(3-4-3) Target Operator

$$U_t + F_x = 0$$

- **SBP matrix form:**

$$D = P^{-1} Q \;;\; P = P^T \;;\; \psi^T P \psi > 0 \;;\; Q + Q^T = Diag[-1,0,\cdots,0,1] \;;$$

- **WENO Stencil Biasing matrix form:**

$$\frac{\boldsymbol{f}^{ES}_{j+1/2} - \boldsymbol{f}^{ES}_{j-1/2}}{\Delta x} = [\delta \bar{\mathbf{x}}]^{-1} \; D_1 \bar{\boldsymbol{f}}^{ES} \qquad D_1 = \begin{pmatrix} -1 & 1 & 0 & \cdots & 0 & 0 \\ 0 & -1 & 1 & 0 & \cdots & 0 \\ 0 & 0 & \ddots & \ddots & 0 & 0 \\ 0 & \cdots & 0 & -1 & 1 & 0 \\ 0 & 0 & \cdots & 0 & -1 & 1 \end{pmatrix}$$

$$f^{ES}_{j+1/2} = \bar{\omega}^L_{j+1/2} \bar{f}^L_{J+1/2} + \bar{\omega}^C_{j+1/2} \bar{f}^C_{J+1/2} + \bar{\omega}^R_{j+1/2} \bar{f}^R_{J+1/2}$$

$$\bar{\boldsymbol{f}}^L = I^L_{fs} \boldsymbol{f} \;;\; \bar{\boldsymbol{f}}^C = I^C_{fs} \boldsymbol{f} \;;\; \bar{\boldsymbol{f}}^R = I^R_{fs} \boldsymbol{f}$$

- **Equating the two forms yields**

$$[\delta \bar{\mathbf{x}}]^{-1} \; D_1 \bar{\boldsymbol{f}}^{ES} = [\delta \bar{\mathbf{x}}]^{-1} \; D_1 \; [\bar{\omega}_t^L I^L_{fs} + \bar{\omega}_t^C I^C_{fs} + \bar{\omega}_t^R I^R_{fs}] \boldsymbol{f} = P^{-1} Q \boldsymbol{f}$$

- **Solve HUGE Matrix Equation and you're done!**

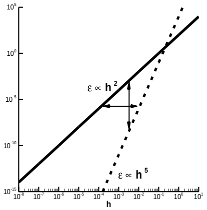

Deriving SBP(3-4-3) Target Operator

$$U_t + F_x = 0$$

$$[\delta \bar{\mathbf{x}}]^{-1} \; D_1 \bar{\boldsymbol{f}}^{ES} = [\delta \bar{\mathbf{x}}]^{-1} \; D_1 \; [\bar{\omega}_t^{\;L} I_{fs}^{L} + \bar{\omega}_t^{\;C} I_{fs}^{C} + \bar{\omega}_t^{\;R} I_{fs}^{R}] \boldsymbol{f} = P^{-1} Q \boldsymbol{f}$$

- **Mathematica could not find solution for uniform meshes**
  - **Inconsistent constraints on system**
  - **Flux mesh must be consistent with P-norm used in proof**
- **Equating two matrices (requires??) nonuniform flux points**

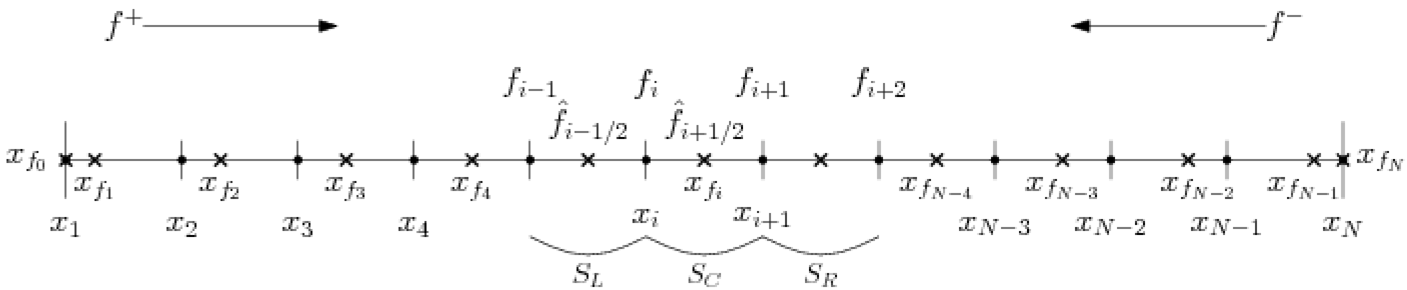

$$\bar{x} = \Delta x \left[0, \frac{43}{144}, \frac{244}{144}, \frac{349}{144}, \frac{7}{2}, \cdots, n-1-\frac{349}{144}, n-1-\frac{244}{144}, n-1-\frac{43}{144}, n-1 \right]$$

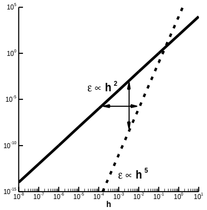

Numerical Results: Finite Domain
Eigenvalues WENO vs. ESWENO

Eigenvalues for finite domain 4th-order case (3-4-3).

$$U_t + F_x = 0 \; ; \; F = aU$$

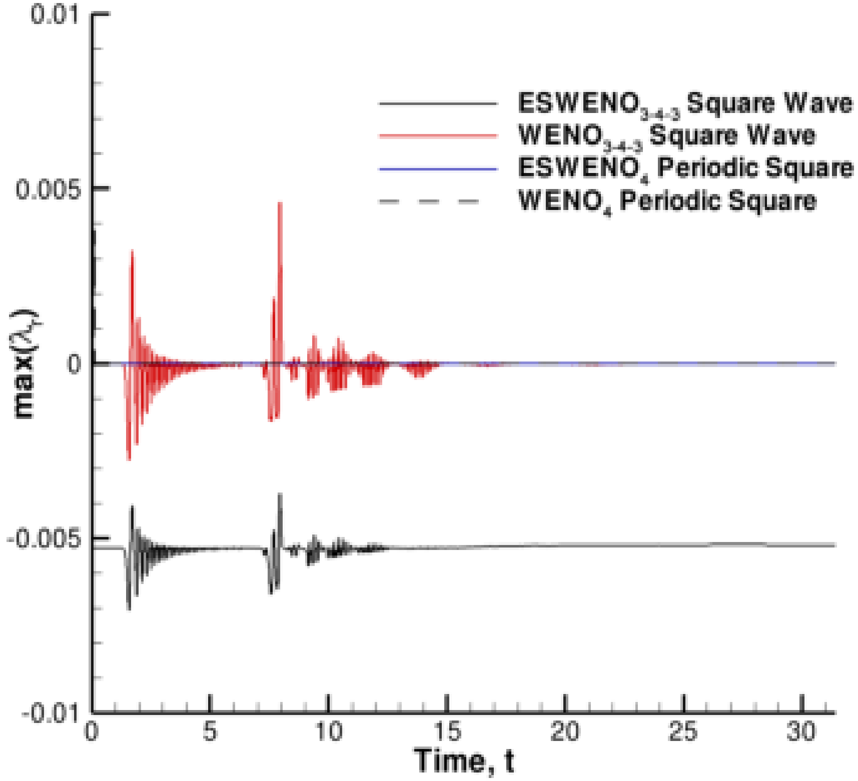

Numerical Results: Finite Domain
Eigenvalues WENO vs. ESWENO

Square Wave coming into domain. ESWENO 4th:(3-4-3)

$$U_t + F_x = 0 \; ; \; F = aU$$

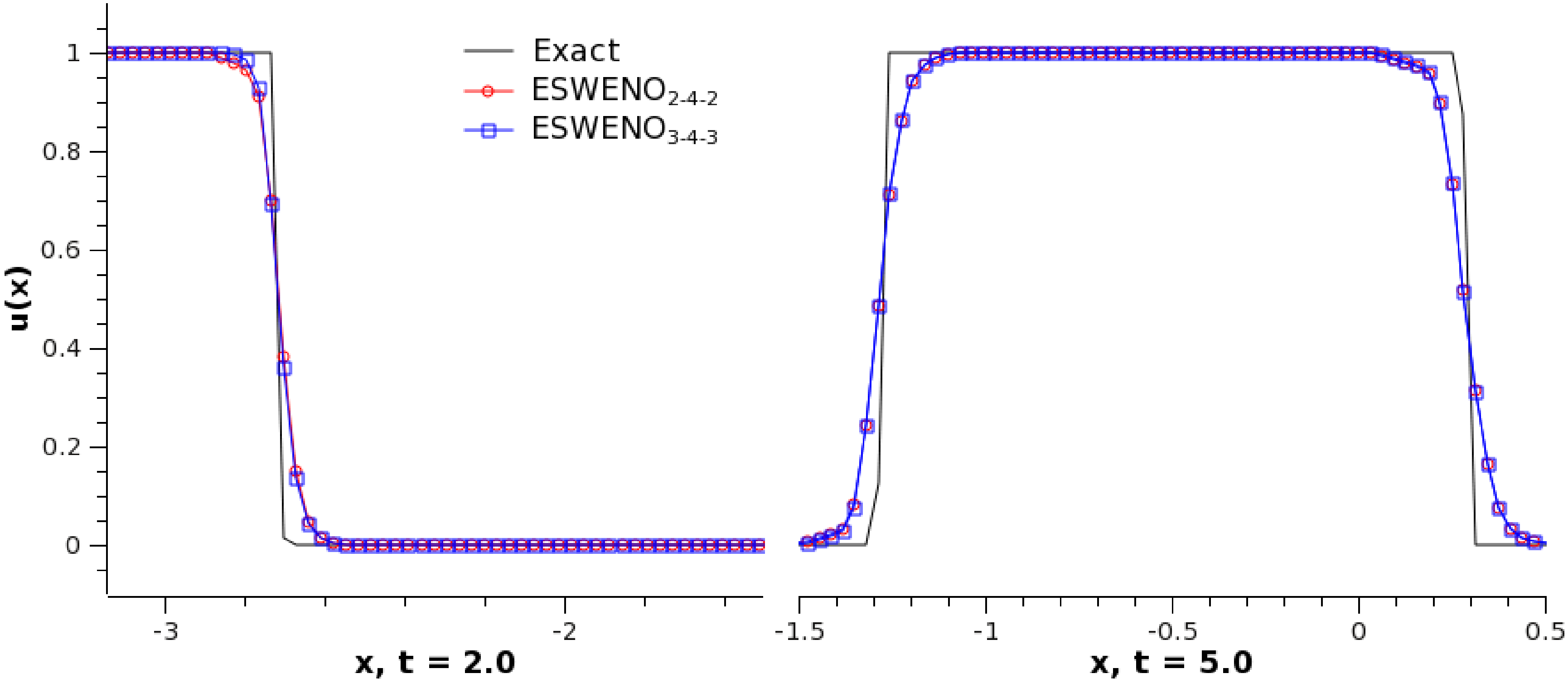

Numerical Results: Finite Domain

Euler isotropic vortex: ESWENO 4th(3-4-3)

	Linear Block Norm		$\text{ESWENO}_{3\text{-}4\text{-}3}$	
Number of Cells	$\mathbf{L_2}$ **Error**	$\mathbf{L_2}$ **Rate**	$\mathbf{L_2}$ **Error**	$\mathbf{L_2}$ **Rate**
50×50	2.49E-05	-	5.32E-05	-
100×100	1.64E-06	3.92	2.25E-06	4.57
200×200	1.04E-07	3.98	1.08E-07	4.37
400×400	6.57E-09	3.99	6.62E-09	4.04

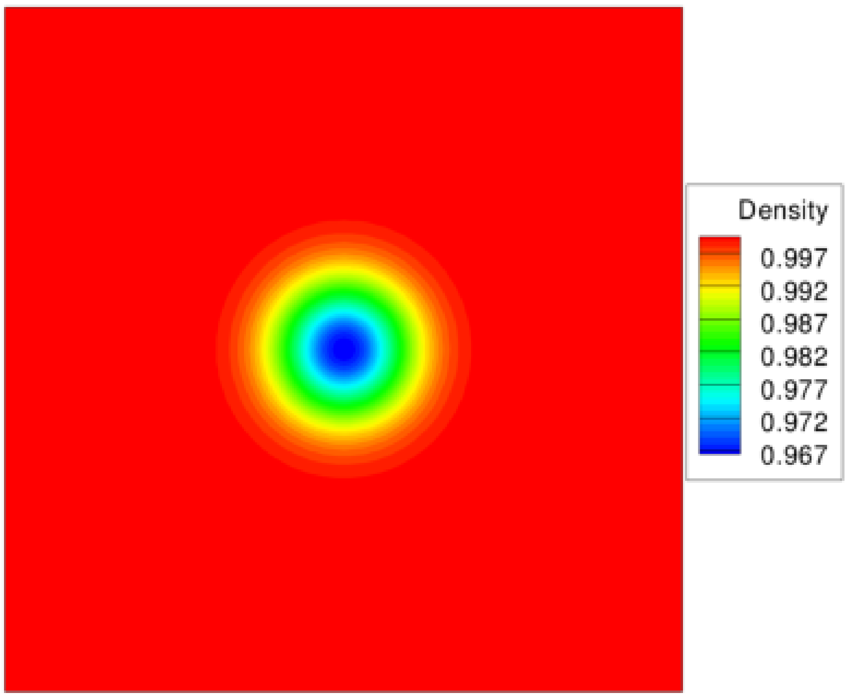

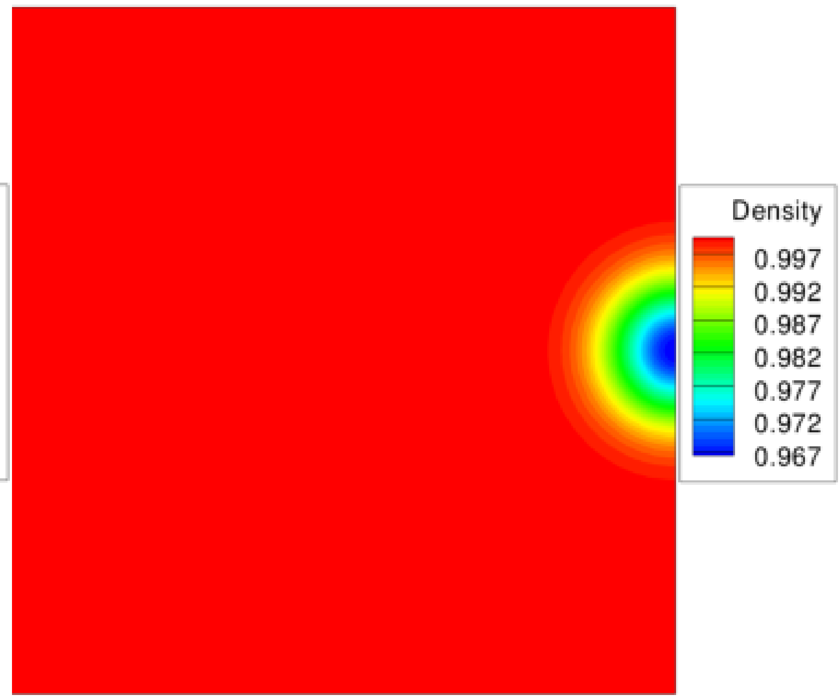

Numerical Results: Finite Domain
4th-order *ESWENO for Chemistry*

Compare Non-reacting and Reacting Mixing Layers

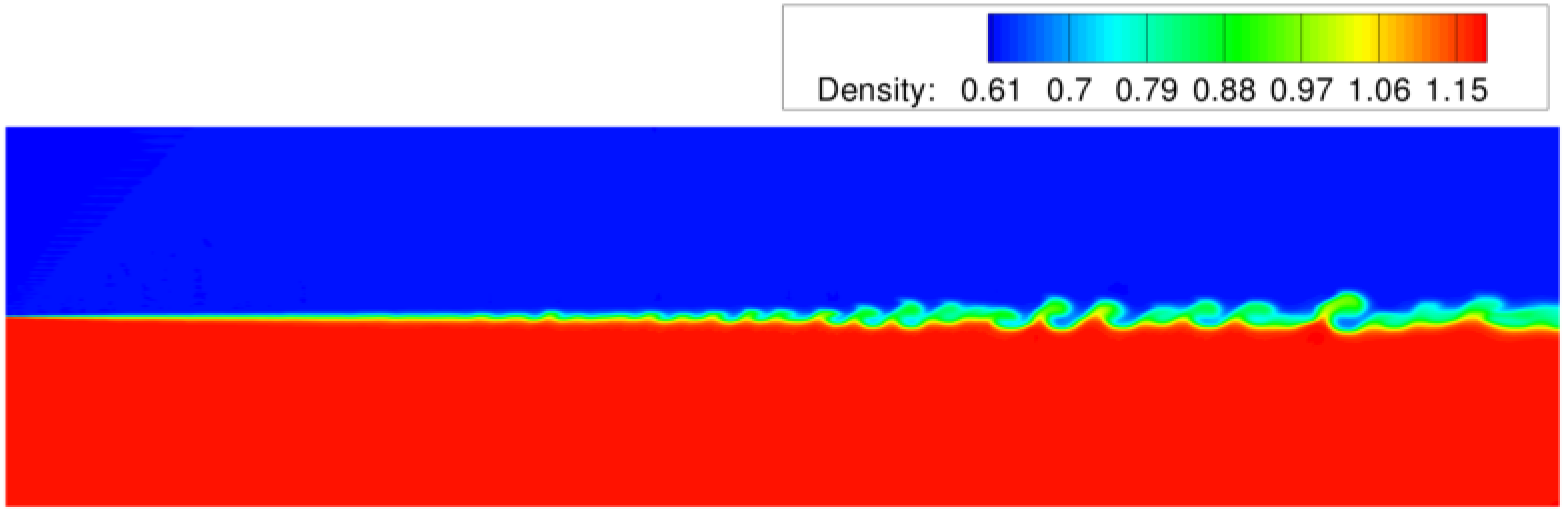

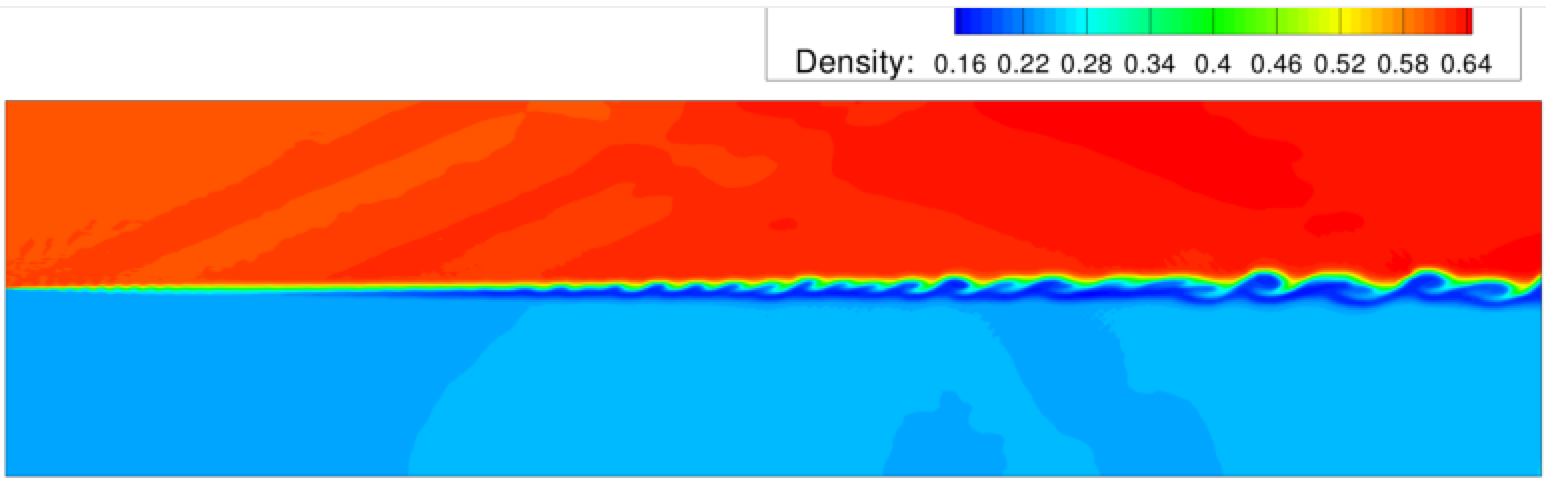

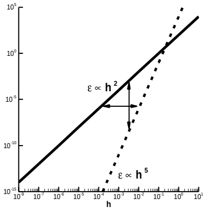

Conclusions

- The systematic methodology for constructing fourth-order ***finite domain Energy Stable WENO schemes*** is developed.
- We prove that for hyperbolic systems, the ***finite domain** ESWENO* scheme is ***stable in the energy norm*** for both continuous and ***discontinuous*** solutions.
- The eigenvalues of the finite domain ESWENO dissipation operator is located in the left-half plane.
- Based on the rigorous truncation error analysis, ***the new weight functions*** are developed, which ***drastically improve the accuracy*** of the ESWENO scheme and provide ***excellent shock-capturing capabilities***
- Numerical experiments show that the new finite domain ESWENO scheme with the new weights outperform the conventional WENO schemes in terms of accuracy.

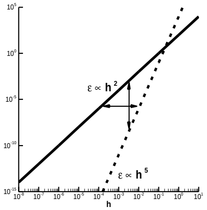

Questions/Comments

- Historical Perspective?
- Discontinuous Galerkin?
- ESWENO?